

**DETERMINATION OF DENSITY OF STATES OF n-
TYPE HYDROGENATED AMORPHOUS SILICON BY
PHASE SHIFT ANALYSIS OF MODULATED
PHOTOCURRENT METHOD**

by

Ferhat Kocabıyık

B.S. in Physics, Boğaziçi University, 1993

Submitted to the Institute for Graduate Studies in
Science and Engineering in partial fulfillment of
the requirements for the degree of
Master of Science
in
Physics



Boğaziçi University

1995

ACKNOWLEDGMENTS

I would like to thank Prof. Dr. Gülen Aktaş for her help and guidance during this thesis. Her valuable criticism and support made this work possible.

I would also like to thank Assoc. Dr. Ender Aktulga for his help and for providing me with the necessary documents.

I would also like to thank my friends, especially Aydın Akkaya, Zuhâl Kaplan, Gültekin Gülşen, Seval Genç, Alparslan Yaradanakul for their help and support during my study in the laboratory.

ABSTRACT

Determination of the energetic distribution of localized states due to random network and structural defects within the mobility gap of amorphous semi conductors is of great importance for understanding the transport properties of these materials. Since there is no structural order, the band states can be only determined experimentally.

In this thesis, the density of states (DOS) distribution in the energy gap of Hydrogenated n-type amorphous silicon is determined. For this purpose a The Phase shift analysis of modulated photocurrent (PSAMP) method is studied. The validity of the PSAMP theorem for the doped a-H:Si is discussed. The theorem is verified for this type of semiconductors and the distribution of the states is determined for a range of 400 meV.

KISA ÖZET

Amorf yarı iletkenlerin mobilite aralığında gelişi güzel ağ örgüsünden ve yapısal bozuklardan ileri gelen yerleşik durumların enerjiye göre dağılıklarının saptanması bu malzemelerin taşıma mekanizmalarının anlaşılması açısından çok önemlidir. Yapısal bir düzen olmadığından bu yerleşik durumlar deney yoluyla belirlenmelidir.

Bu çalışmada, n- tipi hidrojenlendirilmiş amorf silisyum ince filimin enerji bant aralığındaki durum yoğunluğu araştırılmıştır. Bu amaçla module edilmiş foto-akım faz analizi metodundan yararlanılmış ve teoremin geçerliliği tartışılmıştır. Teoremin bu tip yarı-iletkenler için uygun olduğu gözlemlenmiş ve yerleşik durum yoğunluğu 400 meV' lik bir bölgede belirlenmiştir.

TABLE OF CONTENTS

TITLE	II
ACKNOWLEDGMENTS	iii
ABSTRACT	iv
KISA ÖZET	v
TABLE OF CONTENTS	vi
LIST OF FIGURES	ix
LIST OF TABLES	x
LIST OF SYMBOLS	xi
1. INTRODUCTION	1
1.1. A Brief Review of Hydrogenated Amorphous Silicon Films.	2
1.1.1. A Historical Perspective of a-H:Si Films.	2
1.2. The Effect of Hydrogen and Other Additives on the Electronic Properties of Amorphous Silicon.	2
1.2.1. Defects in Amorphous Films.	3
1.2.2. Comparison of Pure and Hydrogenated a-Si.	3
1.2. 3. Dopants.	5
1.3. Preparation of Doped Amorphous Semiconductors.	5
1.3.1. Doping by the Glow Discharge Technique.	5
1.3.2. Hydrogenated Sputtered Amorphous Semiconductors.	6
1.3.3. Doping by Ion Implantation.	6
1.3.4. Doping by Thermal Diffusion.	6
1.3.4. Post-Hydrogenation of CVD Films.	7

1.4. Electronic Structure of Amorphous Solids.	7
1.4.1. Conductivity Mechanism.	7
1.4.2. Common Experimental Techniques Used to Determine the Gap State Density.	9
a. Capacitance Measurements.	9
b. Field Effect Measurements.	9
c. Deep Level Transient Spectroscopy (DLTS).	9
d. The analysis of modulated photocurrent.	10
2. PHASE-SHIFT ANALYSIS OF MODULATED PHOTOCURRENTS.11	
2.1. General Description.	11
2.2. Theory	11
3. EXPERIMENTAL METHOD	23
3.1 Description of the Apparatus	23
3.1.1. Temperature dependent conductivity (IT) measurements.	23
3.1.2 Phase Shift Measurements.	24
3.2 Results of Measurements.	26
3.2.1. Initial Procedure.	26
3.2.2. Results.	26
a. IT Measurement Results.	26
b. Phase Shift Measurement Results.	27
c. The Plot of DOS.	30
d. The data process.	34
4. CONCLUSION	39
APPENDIX A: COMPUTER PROGRAM USED IN THE I-V MEASUREMENTS	40
APPENDIX B: COMPUTER PROGRAM USED IN THE PHASE SHIFT MEASUREMENTS	45
REFERENCES	54

LIST OF FIGURES

FIGURE 1.1. MODEL OF CFO FOR THE DENSITY OF STATES OF AMORPHOUS SEMICONDUCTORS.....	8
FIGURE 2.1. SCHEMATIC ENERGY DIAGRAM ACCEPTED BY PSAMP THEORY.....	12
FIGURE 2.2. $G_1(E)$ VERSUS ENERGY GRAPH.....	18
FIGURE 2.3. $G_2(E)$ VERSUS ENERGY GRAPH.....	20
FIGURE 3.1. IT SETUP DIAGRAM.....	23
FIGURE 3.2. SETUP DIAGRAM FOR PHASE-SHIFT MEASUREMENTS.....	25
FIGURE 3.3. LOG(I) VERSUS 1000/T GRAPH.....	27
FIGURE 3.4. THEORETIC AND EXPERIMENTAL PHOTOCURRENT VERSUS MODULATION FREQUENCY GRAPH FOR T=333 K.....	28
FIGURE 3.5. THEORETIC AND EXPERIMENTAL PHOTOCURRENT VERSUS MODULATION FREQUENCY GRAPH FOR T=313 K.....	28
FIGURE 3.6. THEORETIC AND EXPERIMENTAL PHOTOCURRENT VERSUS MODULATION FREQUENCY GRAPH FOR T=293 K.....	28
FIGURE 3.7. THEORETIC AND EXPERIMENTAL PHOTOCURRENT VERSUS MODULATION FREQUENCY GRAPH FOR T=268 K.....	29
FIGURE 3.8. THEORETIC AND EXPERIMENTAL PHOTOCURRENT VERSUS MODULATION FREQUENCY GRAPH FOR T=263 K.....	29
FIGURE 3.9. THEORETIC AND EXPERIMENTAL PHOTOCURRENT VERSUS MODULATION FREQUENCY GRAPH FOR T=248 K.....	30
FIGURE 3.10. THE DENSITY OF STATES VERSUS ENERGY GRAPH, T=333 K.....	30
FIGURE 3.11. THE DENSITY OF STATES VERSUS ENERGY GRAPH, T=313 K.....	31
FIGURE 3.12. THE DENSITY OF STATES VERSUS ENERGY GRAPH, T=293 K.....	31
FIGURE 3.13. THE DENSITY OF STATES VERSUS ENERGY GRAPH, T=268 K.....	32
FIGURE 3.14. THE DENSITY OF STATES VERSUS ENERGY GRAPH, T=263 K.....	32
FIGURE 3.15. THE DENSITY OF STATES VERSUS ENERGY GRAPH, T=248 K.....	33
FIGURE 3.16. GAMMA VERSUS FREQUENCY GRAPH.....	35
FIGURE 3.17. ω VERSUS 1/T GRAPH.....	36
FIGURE 3.18. DOS VERSUS ENERGY GRAPH.....	37
FIGURE 3.19. DOS VERSUS ENERGY GRAPH.....	38

LIST OF TABLES

TABLE 1.1. A COMPARISON OF THE PROPERTIES OF THE NOMINALLY PURE AND HYDROGENATED AMORPHOUS SILICON	4
---	---

LIST OF SYMBOLS

n	Concentration of free electrons
n_d	Dark free electron concentration
$m(E)$	Trapped electron concentration
$M(E)$	Density of energy states
v	Thermal velocity
	Capture crosssection for electron
N_c	Density of states of conduction band
T	Temperature
E_d	Demarcation energy level
I	Photon absorption rate

1. INTRODUCTION

During the last decades interest in both fundamental and applied aspects of amorphous semiconductors has grown rapidly. In the last years, the development of amorphous semiconductor technology promised an application area for solar cells, thin film transistors, electrophotographic copiers, laser printers, computer memories and myriad of other devices.

In April 1967 a short explanatory study of glow discharge deposited silicon was undertaken [1,2], followed in 1968, by a similar exercise on Germanium [2]. Initially the objective was to assess the feasibility of using these materials for the fabrication of thin film devices such as resistors and thermistors, but soon after growing interest in amorphous semiconductors showed itself as today's technology.

Before any analysis of the physical properties of an amorphous solid can be undertaken, a knowledge of the band structure is essential. However, because of lack of long range periodicity in amorphous materials, it is much more difficult to determine structure theoretically. The band structure can only be determined experimentally.

The commonly used experimental methods for exploring the electronic structure of amorphous materials are the Field Effect [3,4], DLTS and C-V methods [5,6] all which require an interface with the semiconductor material, therefore there is a danger of determining surface states rather than the bulk states. In this work another method which is proposed by H. Oheda [7] is used to investigate the electronic structure of the material under consideration. In this method no interface is required, bulk material is measured directly.

In contrast to above mentioned methods based on the analysis of a steady state phenomenon, this method which utilizes a transient method, is based on an analysis of the phase shift of the modulated photocurrent as the modulation frequency of an exciting light that varies. The Density of States (DOS) structure is then shown to be directly related to the induced phase shift.

The aim of our work was to apply this PSAMP (Phase Shift Analysis of Modulated Photocurrent) method to phosphorus doped a-H:Si films. We have determined the DOS within the mobility gap in an energy range of about 400 meV below the conduction band. A brief review of hydrogenated amorphous silicon films is given in the first chapter. Second chapter deals with the theory of PSAMP. Next chapter details experimental method and results and in the last chapter a discussion part is presented.

1.1. A Brief Review of Hydrogenated Amorphous Silicon Films.

1.1.1. A Historical Perspective of a-H:Si Films.

The role of Hydrogen in a-H:Si was appreciated much later on than this films first investigated. Pure or non-hydrogenated films are known to contain many dangling bonds that create a large density of localized states throughout the energy gap of the semiconductor. The role of hydrogen in these films is to terminate these broken bonds and consequently remove many states from the energy gap.

For many years it had been thought to be a basic and fundamental fact that an amorphous semiconductor couldn't be substitutionally doped. Mott had explained in a simple and intuitive way that the absence of a periodic steric constraints in a disorder system could allow the normal valency of any impurity atom to be completely satisfied. This is the usual mechanism for introducing extra electrons and holes into a solid could be tremendously impeded.

Nevertheless in 1975 W.E. Spear and P.G. Lecomber demonstrated a new amorphous silicon material which could be doped both n type and p type and its room temperature conductivity could be made to vary over more than ten orders of magnitude. It was discovered that a very important feature of this material was that it contained a significant amounts of bonded hydrogen.

1.2. The Effect of Hydrogen and Other Additives on the Electronic Properties of Amorphous Silicon.

One can group three types of additives for the concept of the electronic properties of a-Si in terms of their effects;

1. Dangling and other weak bonds
2. Hydrogen and other bond terminators
3. n- and p- type of dopands

Although dangling bonds are not generally thought as additives, conceptually they can be viewed as extrinsic to a perfect continuous random network and therefore, as something added to that as yet unobtainable ideal.

For the second case by design, Hydrogen, Oxygen and more recently Fluorine have been used as band terminators to passivate the extrinsic effects of dangling bonds.

Finally for the last case Phosphorus and Boron are commonly added to a-Si:H to make n and p type amorphous semiconductors. The doped materials are employed in diodes, transistors and other configurations of device potential.

1.2.1. Defects in Amorphous Films.

Defects in amorphous semiconductors probably result from strain-relief mechanism and from bonding misfits during the growth process. Except for a-As these materials contain group IV elements as major constituents which cannot undergo valence alternation. A variety of paramagnetic and diamagnetic defects have been proposed and discussed by Adler[9] for a-Si and a-Si:H. The overconstrained nature of amorphous films suggests that the defects may not be randomly distributed but could be predominantly located at internal voids and strain-relief interfaces between low-strain regions. At the present state of our knowledge of covalent amorphous semiconductors following points appear to be able to cover the defect concept;

1. Well defined defects exists in covalent amorphous semiconductors.
2. These ordinary control the equilibrium transport properties of the material via the position of Fermi level.
3. They can also be expected to control the trapping and recombination kinetics.
4. Several different types of defect centers can be simultaneously present.
5. The defect centers can be either charged or neutral.

1.2.2. Comparison of Pure and Hydrogenated a-Si.

Table 1.1 lists the comparative properties of interest for nominally pure and hydrogenated a-Si. By nominally pure is meant a-Si prepared by clean evaporation or by sputtering or ion bombardment with an inert species such as Argon[8]. Except for the inert species, and perhaps some residual C or O at or below concentrations of order 0.1 atomic percent, such preparations give pure a-Si. The column labeled hydrogenated refers to a product of the glow discharge decomposition of silane or the reactive sputtering of Si with a hydrogen bearing plasma.

Table 1.1. A comparison of the properties of the nominally pure and hydrogenated amorphous silicon.

	<i>PURE</i>	<i>HYDROGENATED</i>
DANGLING BONDS	$5 \times 10^{19} \text{ cm}^{-3}$	$< 10^{16} \text{ cm}^{-3}$
STATES IN THE GAP	$10^{19} - 10^{20} \text{ cm}^{-3} \text{ eV}^{-1}$	$10^{16} - 10^{17} \text{ cm}^{-3} \text{ eV}^{-1}$
CONDUCTIVITY	Hopping at fermi level $\exp(-(T_0 / T)^{1/4})$ at RT	Activated to band or band tail $\exp(\Delta E / kT)$ at RT
OPT. ABSORPTION	Tails into infrared	Edge near 1.7 eV
DOPING EFFECTS	Not discernible	p or n type, conductivity changes up to 10^{10} times
PHOTORESPONCE	None	Photoconductive

The first difference we note is that the number of dangling bonds ($5 \times 10^{19} \text{ cm}^{-3}$) and the number of gap states $10^{19} - 10^{20} \text{ cm}^{-3} \text{ eV}^{-1}$ in pure a-Si are both reduced by orders of magnitude in a-Si:H [10]. As a consequence the $\exp(-(T_0 / T)^{1/4})$ the Mott Law hopping conductivity attributable to carrier transport within the band gap is the dominant near room temperature conductivity mechanism in pure a-Si. For a-Si:H an activation energy, characteristic of carrier activation to a band or band tail conduction path is observed [11]. For undoped a-H:Si, values of activation energy greater than $\approx 1.0 \text{ eV}$ have been observed [12].

To first approximation, the differences enumerated in Table 1.1 are explainable merely by the passivation role of H as a dangling bond terminator. Along with the removal of dangling bond states from the gap, the dominant conductivity and absorption processes are now associated with near band edge states or inter-bond transitions between them. Presumably the because in-gap states which acted as rapid non-radiative recombination centers in pure a-Si are no longer present after Hydrogenation, observable life times, even as long as milliseconds, are possible for photo-excited carriers that participate in, for example, photoconduction. Finally when whit the reduction of the gap states, the addition of reasonable concentrations of dopands such as P or B can move the Fermi level and give either n or p type a-Si:H, respectively.

1.2. 3. Dopants.

The conventional view [13] of doping in a semiconductor, and the view that has carried over as a first approximation to doped a-Si:H is that trivalent and pentavalent dopants (e.g., B and P respectively) are incorporated substitutionally for Si with four-fold coordination. Therefore B and P atoms are, respectively acceptors and donors in a-Si:H. The host atomic structure or band structure are assumed to be negligibly changed by the presence of dopants. Within the host band gap, the Fermi level is presumed to move according to how many electrical active donors (or acceptors) are present relative to the background density of states $N(E)$ at Fermi energy level. In a typical case, for low doping levels, electrical activity of about 1/4 the donors could account for the movement of the Fermi level if the background DOS were of order $N(E_f) \approx 10^{17} \text{ eV}^{-1} \text{ cm}^{-3}$ for Fermi energy level near midgap. For the heavily doped case, impurity bands and new conduction paths are believed to occur [14,15].

1.3. Preparation of Doped Amorphous Semiconductors.

A review of the methods by which doped amorphous semiconductors have been prepared has been published before [16] and therefore only a brief discussion will be given here. Essentially five techniques have been used to date, namely glow discharge deposition, ion implantation, rf sputtering, thermal diffusion and post-hydrogenated CVD, and in the following we shall consider each of these in turn.

1.3.1. Doping by the Glow Discharge Technique.

This technique has received a considerable amount of attention in recent years since it was used in the first successful doping experiments on amorphous Si and Ge by Spear and Lecomber in 1975 [15,17]. Thin film specimens of a-Si or a-Ge were formed by decomposing the corresponding hydride, Silane or Germane, in a radio frequency field. The power level is small, typically a few watts, and frequencies between 1 and 100 Mhz have been tried. The electronic properties of the deposited specimens are critically dependent on a number of variables such as the temperature of the substrate during deposition [18], flow rate, gas pressure, rf power level and the geometry of the reaction tube. Doping from the gas phase can be achieved by adding small but accurately determined amounts of Phosphine or Diborane to the Silane.

1.3.2. Hydrogenated Sputtered Amorphous Semiconductors.

The work of Harvard group on hydrogenated sputtered a-Ge and Si has made an important contribution to the subject. It is generally accepted that specimens prepared by cathodic sputtering contain a high overall level of gap states associated with dangling bonds in probably quite an extensive microvoid structure. Poul and his collaborators [19,20] showed that by adding hydrogen to the argon used in sputtering process, a few atomic percent of hydrogen can be incorporated into the films. This has a marked effect on the electronic properties of the material, greatly reduces the ESR signal [21], and is consistent with the suggestion that dangling bonds have been saturated by hydrogen atoms. In the present context, the significant result is that fairly sensitive doping from the gas phase using Phosphine and Diborane now becomes possible [22].

1.3.3. Doping by Ion Implantation.

Doping by ion implantation has achieved considerable importance in crystalline device technology. Although earlier attempts with evaporated a-Ge were not encouraging, recent work on glow discharge a-Si has shown that is possible to dope this material by implantation of the substitutional impurities P, As, Sb, Bi, B, Al, Ga, In, Tl, and the interstitial impurities Na, K, Rb and Cs [23,24,25,26]. Implantation doping provides the same range of control of the electrical properties as gas-phase glow discharge doping, but at lower doping efficiency. Compensation of pre-doped specimens by ion implantation has been investigated, found to be feasible and predictable, and used for the production of implanted a-Si p-n junctions.

1.3.4. Doping by Thermal Diffusion.

Beyer and Fisher [27] have doped glow discharge a-Si interstitially with Li both by thermal diffusion and by ion implantation. For the former, a layer of Li was evaporated onto the undoped material and then heated for one hour to allow the Li to diffuse in to the sample. Under this conditions the diffusion length is likely to be greater than the sample thickness so that a homogenous distribution is obtained.

1.3.4. Post-Hydrogenation of CVD Films.

Recently two research groups [28,29] have doped a-Si Films prepared by chemical vapor decomposition of mixtures of Silane, hydrogen and impurity gases at high temperature (850 K). Technique is not easy since the annealing stage can result in plasma etching and loss of the film. Furthermore it is difficult to diffuse into the a-Si a uniform Hydrogen concentration of sufficient magnitude to produce a material with good electronic properties.

1.4. Electronic Structure of Amorphous Solids.

1.4.1. Conductivity Mechanism.

Although band tails can have very significant effects on the electronic properties of amorphous semiconductors, the lack of applicability of Bloch's theorem has much more profound consequences for transport. In the absence of long-range order, it is possible that all electronic states are localized in the vicinity of a particular atom. Mott [30] proposed that a critical density of states exists above which all states exhibit a finite mobility for free carriers even at absolute zero temperature; this critical density has been called the mobility edge.

Cohen et al. [31] assumed the existence of band tails and mobility edges, and suggested that for multicomponent amorphous solids the valence and conduction band tails could overlap in the center of the gap, thus yielding a finite density of states at the Fermi energy, $g(E_f)$. Cohen, Fritzsche, Ovshinsky (CFO) model, sketched in Fig 1.1, provides a useful structure for the analysis of transport and optical data.

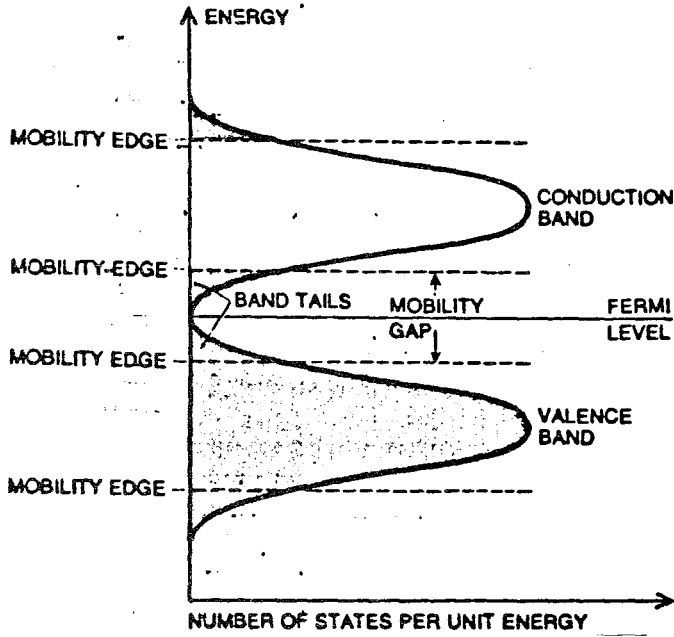


Figure 1.1. Model of CFO for the density of states of covalent amorphous semiconductors.

The most straightforward manifestation of a sharp mobility edge would be an electrical conductivity which varies as

$$\sigma = N_c e \mu_e \exp[-(E_c - E_f)\beta] + N_v \mu_h \exp[-(E_f - E_v)\beta] \quad (1.1)$$

where N_c and N_v are the effective densities of states in the conduction and valance bands, μ_n and μ_h are the electron and hole mobilities beyond the mobility edges, respectively.

Mott [32] pointed out that for a sufficiently large $g(E_f)$, phonon assisted hopping among localized states near Fermi energy level might well predominate band-like conduction beyond the mobility edges at sufficiently low temperatures. Mott further suggested that at very low temperatures, when very few energetic phonons are present, such hopping conduction would take place preferentially to farther rather than a nearest-neighboring localized states, in order to reduce the energy that must be obtained from the phonons. Mott showed that for this mechanism of variable range hopping conduction, the conductivity varies as,

$$\sigma = \sigma_0 \exp\left[-\left(\frac{T_0}{T}\right)^{\frac{1}{4}}\right] \quad (1.2)$$

where σ_0 and T_0 are constants. When amorphous silicon hydrogenated either during deposition or afterwards expected behavior is small density of unpaired spins (few dangling bonds), no variable-range hopping and sharp absorption edge or namely a band model similar to CFO .

1.4.2. Common Experimental Techniques Used to Determine the Gap State Density.

To date there is no technique which gives a reliable comprehensive description of the density of states of a-Si:H. The measurement of the gap state density is especially difficult in undoped material. This [33] section will review briefly the techniques for evaluation of gap state density in a-Si:H.

a. Capacitance Measurements. In amorphous semiconductors, the standard formulae for junction capacitance of metal-crystalline Si barriers cannot be used because of the relatively large density of localized states which contribute to the space charge in the depletion region. Using an assumed density of states, the capacitance variation with voltage and frequency and the barrier profile can be calculated, but the interpretation of the density of states measurements is not unique. For example, in the case where measurement of the capacitance variation of Schottky barriers with a number of parameters is involved, there are such a significant number of assumptions and errors in calculating certain parameters that capacitance data cannot be relied upon by itself to provide useful information to determine the correlation between density of states and barrier profile.

b. Field Effect Measurements. This technique was the earliest method used to measure the density of states in a-Si:H. Although it has been ameliorated and refined over the years, measurements based on this technique have often caused several debates concerned with differentiating surface and bulk properties. It has also been demonstrated that there is no unique solution to the field effect data and the detailed differences in derived density of states, particularly near the density of states minimum, should be treated with caution. In conclusion, because of the problem of separating surface states from bulk states, field effect measurements only reveal a maximum for the density of bulk states.

c. Deep-Level Transient Spectroscopy (DLTS). DLTS is a powerful technique which has been used extensively to analyze defects in crystalline semiconductors. Both current and capacitance DLTS have been used to study a-Si:H.

The current or capacitance transients are measured often as a function of temperature following a trap filling event in a Schottky barrier or $p-n$ junction. Optical excitation or injection forward-biasing is used to fill traps at low temperatures and the current or capacitance transient due to trap emptying is measured at fixed time intervals after the diode is returned to a reverse bias condition. The temperature is scanned and the difference in current at times t_1 and t_2 of the transient are recorded and plotted against temperature revealing peaks in the spectrum. The energy depth and concentration of traps can then be calculated but an important assumption made in DLTS is that the motion of the charge is emission rate limited. Thus, any long retrapping event (long compared with emission time) would lead to an underestimation of the trap density. The application of DLTS to materials containing a continuous distribution of states is very difficult. On the other hand, capacitance DLTS cannot be made on low conductivity undoped material, thus their studies are restricted to doped material where the detailed density of states will probably be different from undoped material. In addition, in order for the detailed spectrum to reflect accurately a density of states, the signal should be saturated over the entire spectrum in order to ensure that the traps are completely full. This is sometimes not easily observed at the minima of the DLTS signal, which corresponds to the much quoted minimum in the density of states. In addition, a detailed understanding of the Schottky or junction devices is necessary in order for the DLTS to provide useful information. It is certain that in the future this technique may provide some very useful data; however, no systematic data on undoped a-Si:H has emerged yet.

d. The Analysis of Modulated Photocurrent. Phase-shift analysis of modulated photocurrent [34] yields information about the energetic structure of gap states above midgap. But theory has constraints, e.g., band to band conduction, trapping of mobile electrons etc. This method is detailed in next chapter.

2. Phase-Shift Analysis of Modulated Photocurrents.

2.1. General Description.

Photocarriers in an a-Si:H sample are generated band to band by sinusoidally modulated light and the resulting photocurrent is measured in terms of amplitude and phase lag with respect to the excitation signal as a function of modulation frequency. Thus in principle, the physical processes involved are similar to transient experiments, where excess charge carriers are optically generated by a light pulse and their return to equilibrium is monitored as a function of time. In transient experiments the energy range for which the DOS can be evaluated is given by experimentally accessible time window (limited to short times by the response time of the measurement circuit and to long times by the fast decays of transient signals). Use of lock-in techniques in the frequency domain with improved signal-to-noise ratios allow by orders of magnitudes smaller excitations and thus lower deviation from dark thermal equilibrium. Possible structural changes by light during the measurements can be kept to a minimum. Possible non-linearities of the sample response, e.g., electron-electron interactions or trap saturation, are also expected to be smaller.

Dark currents as well as currents due to other effects like field redistribution (dielectric relaxation) are screened out by the lock-in technique provided that they do not have periodical contributions at the modulation frequency.

2.2. Theory

We will solve the rate equations for charge carriers by assuming the conditions satisfied outlined below;

1. band-to-band generation of mobile carriers
2. trapping of mobile electrons, n_c , into localized states $M(E)$
3. remission of trapped electrons $m(E)$, to the transport path
4. recombination of electrons at the back contact

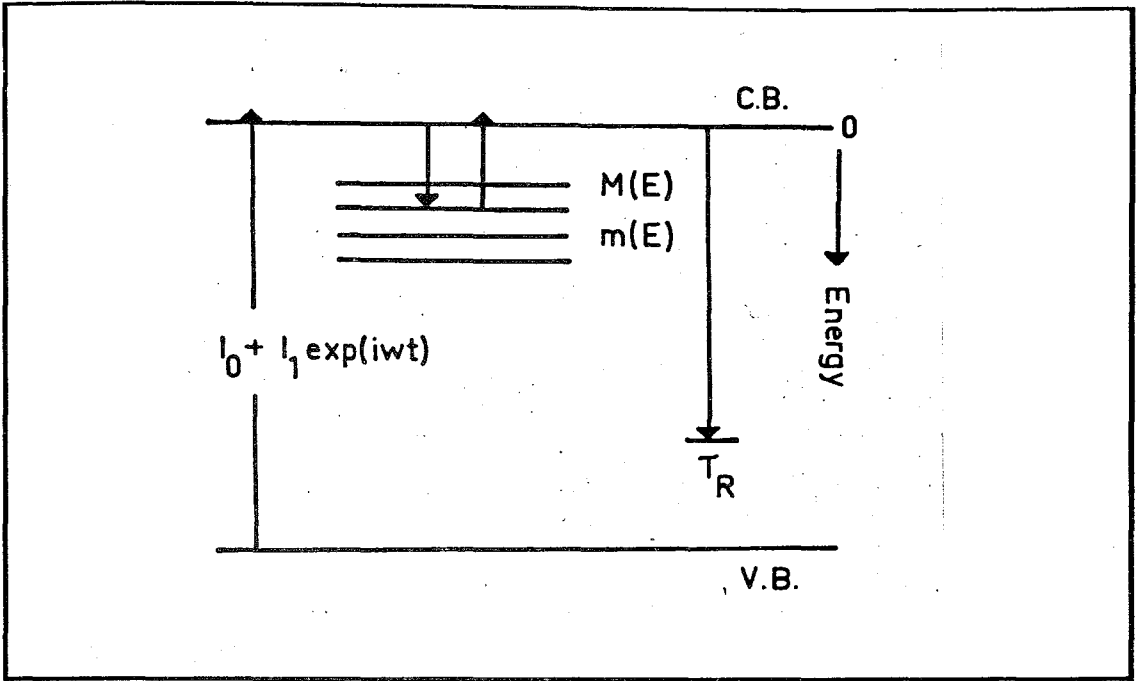


figure 2.1. Schematic Energy Diagram accepted by PSAMP theory.

The rate equations for electrons at the transport path and in the trap states can be written as;

$$\frac{dn}{dt} = I_0 + I_1 e^{i\omega t} - \int_0^{E_d} \frac{dm(E)}{dt} dE - \frac{n - n_d}{\tau_R} \quad (2.1)$$

$$\frac{dm(E)}{dt} = n(M(E) - m(E))\nu\sigma - m(E)\nu\sigma N_c e^{-E/\beta} \quad (2.2)$$

Solutions are expected to be in the form

$$n = n_0 + n_1 e^{i\omega t} \quad (2.3)$$

$$m(E) = m_0(E) + m_1(E) e^{i\omega t} \quad (2.4)$$

put (2.3) into (2.1)

$$n_1 i\omega \exp(i\omega t) = I_0 + I_1 \exp(i\omega t) - \int_0^{E_d} m_1(E) i\omega \exp(i\omega t) dE - \frac{n_0 + n_1 \exp(i\omega t) - n_d}{\tau_R} \quad (2.5)$$

for $\omega=0$ or $I_1 = n_1 = 0$

$$I_0 = \frac{n_0 - n_d}{\tau_R} \quad (2.6)$$

for $\omega \neq 0$, use (2.6) in (2.5)

$$n_1 i \omega e^{i\omega t} = \frac{n_0 - n_d}{\tau_R} + I_1 e^{i\omega t} - \int_0^{E_d} m_1(E) i \omega e^{i\omega t} dE - \frac{n_0 - n_d}{\tau_R} - \frac{n_1 e^{i\omega t}}{\tau_R} \quad (2.7)$$

$\frac{n_0 - n_d}{\tau_R}$ and exponential terms cancel out

$$i \omega n_1 = I_1 - \int_0^{E_d} i \omega m_1(E) dE - \frac{n_1}{\tau_R} \quad (2.8)$$

Now consider second rate equation (2.2) and expected solution type (2.4), use (2.4) in (2.2) by taking its derivative;

$$m_1(E) i \omega \exp(i\omega t) = \left[M(E) - m_0(E) - m_1(E) \exp(i\omega t) \right] \nu \sigma \left[n_0 + n_1 \exp(i\omega t) \right] - N_c \nu \sigma \left[m_0(E) + m_1(E) \exp(i\omega t) \right] \exp(-E\beta) \quad (2.9)$$

Again for $\omega=0$ and $n_1 = m_1(E) = 0$ and $\frac{dm(E)}{dt} = 0$ from (2.9) one can obtain $m_0(E)$ through steps below;

$$0 = n_0 \nu \sigma \left[M(E) - m_0(E) \right] - \nu \sigma N_c m_0(E) \exp(-E\beta) \quad (2.9.1)$$

$$n_0 \left[M(E) - m_0(E) \right] = N_c m_0(E) \exp(-E\beta) \quad (2.9.2)$$

finally;

$$m_0(E) = \frac{M(E)}{1 + \frac{N_c \exp(-E\beta)}{n_0}} = \frac{M(E) n_0}{n_0 + N_c \exp(-E\beta)} \quad (2.10)$$

Now use (2.10) in (2.9) to get;

$$i\omega m_1(E)e^{i\omega t} = \nu\sigma \left\{ \begin{array}{l} \left[n_0 + n_1 e^{i\omega t} \right] \left[M(E) - \frac{n_0 M(E)}{n_0 + N_c \exp(-E\beta)} - m_1(E)e^{i\omega t} \right] - \\ N_c \exp(-E\beta) \left[\frac{n_0 M(E)}{n_0 + N_c \exp(-E\beta)} + m_1(E)e^{i\omega t} \right] \end{array} \right\} \quad (2.10.1)$$

$$i\omega m_1(E)e^{i\omega t} = \nu\sigma \left\{ \begin{array}{l} \left[n_0 + n_1 e^{i\omega t} \right] \left[\frac{M(E)N_c \exp(-E\beta)e^{i\omega t}}{n_0 + N_c \exp(-E\beta)} - m_1(E)e^{i\omega t} \right] - \\ N_c \exp(-E\beta) \left[\frac{n_0 M(E)}{n_0 + N_c \exp(-E\beta)} + m_1(E)e^{i\omega t} \right] \end{array} \right\} \quad (2.10.2)$$

Expanding the terms one gets;

$$i\omega m_1(E)e^{i\omega t} = \nu\sigma \left\{ \begin{array}{l} m_0 N_c \exp(-E\beta) - n_0 m_1(E)e^{i\omega t} + \frac{n_1 M(E)N_c \exp(-E\beta)e^{i\omega t}}{n_0 + N_c \exp(-E\beta)} - \\ n_1 m_1(E)e^{2i\omega t} - N_c \exp(-E\beta)m_0(E) - m_1(E)N_c \exp(-E\beta)e^{i\omega t} \end{array} \right\} \quad (2.10.3)$$

After cancellations equation ends up with;

$$i\omega m_1(E)e^{i\omega t} = \nu\sigma \left\{ -n_1 m_1(E)e^{i\omega t} + \frac{n_1 M(E)N_c \exp(-E\beta)e^{i\omega t}}{n_0 + N_c \exp(-E\beta)} - n_1 m_1(E)e^{2i\omega t} - m_1(E)N_c \exp(-E\beta)e^{i\omega t} \right\} \quad (2.11)$$

If we divide last equation (2.11) by $m_1(E)e^{i\omega t}$

$$i\omega = \nu\sigma \left\{ -n_0 + \frac{n_1 M(E)N_c \exp(-E\beta)}{m_1(E)(n_0 + N_c \exp(-E\beta))} - n_1 e^{i\omega t} - N_c \exp(-E\beta) \right\} \quad (2.12)$$

by remembering $n = n_0 + n_1 e^{i\omega t}$ (2.12) turns out to be

$$i\omega = \nu\sigma \left\{ \frac{n_1 M(E)N_c \exp(-E\beta)}{m_1(E)(n_0 + N_c \exp(-E\beta))} - n - N_c \exp(-E\beta) \right\} \quad (2.13)$$

After arranging the division in the parenthesis (2.13) one gets

$$i\omega + \nu\sigma n + \nu\sigma N_c e^{-E\beta} = \frac{n_1 \nu\sigma}{m_1(E)} \left(M(E) - \frac{n_0 M(E)}{n_0 + N_c e^{-E\beta}} \right) \quad (2.14)$$

Finally remembering the equation (2.10) one replaces the parenthesis in the last equation (2.14) by (2.10) and obtains;

$$i\omega + \nu\sigma n + \nu\sigma N_c e^{-E\beta} = \frac{n_1 \nu\sigma}{m_1(E)} (M(E) - m_0(E)) \quad (2.14.1)$$

$$\therefore m_1(E) = \frac{n_1 \nu\sigma (M(E) - m_0(E))}{i\omega + N_c \nu\sigma e^{-E\beta} + n \nu\sigma} \quad (2.15)$$

Now remember the equation (2.8), dividing it by n_1 , rearranging the terms and using (2.15) in it, (2.8) becomes;

$$i\omega = \frac{I_1}{n_1} - i\omega \int_0^{E_d} \frac{\nu\sigma (M(E) - m_0(E))}{i\omega + \nu\sigma (n + N_c e^{-E\beta})} dE - \frac{1}{\tau_R} \quad (2.15.1)$$

After a little bit algebra one gets;

$$\frac{I_1}{n_1} = i\omega \left[1 + \int_0^{E_d} \frac{\nu\sigma (M(E) - m_0(E))}{i\omega + \nu\sigma (n + N_c e^{-E\beta})} dE \right] + \frac{1}{\tau_R} \quad (2.16)$$

Now consider the integration term in which has a complex part, carry the complex part from denominator to numerator by multiplying denominator by its complex conjugate.

$$\frac{\nu\sigma (M(E) - m_0(E))}{i\omega + \nu\sigma (n + N_c e^{-E\beta})} = \frac{\nu\sigma (M(E) - m_0(E)) [\nu\sigma (n + N_c e^{-E\beta}) - i\omega]}{(\nu\sigma)^2 (n + N_c e^{-E\beta})^2 + \omega^2} \quad (2.17)$$

If we use (2.17) in (2.16) we obtain a new representation of $\frac{I_1}{n_1}$ in the form A+Bi

$$\frac{I_1}{n_1} = \frac{i}{\tau_R} + i\omega + \int_0^{E_d} \frac{(M(E) - m_0(E)) (\omega)^2 (n + N_c e^{-E\beta}) i\omega}{(\omega)^2 (n + N_c e^{-E\beta})^2 + \omega^2} dE + \int_0^{E_d} \frac{\omega^2 \nu\sigma (M(E) - m_0(E))}{(\omega)^2 (n + N_c e^{-E\beta})^2 + \omega^2} dE \quad (2.17.1)$$

Try to reshape in the form of A+iB

$$\frac{I_1}{n_1} = \frac{1}{\tau_R} + \omega^2 \nu\sigma \int_0^{E_d} \frac{(M(E) - m_0(E))}{(\omega)^2 (n + N_c e^{-E\beta})^2 + \omega^2} dE + i\omega \left[1 + \int_0^{E_d} \frac{(M(E) - m_0(E)) (\omega)^2 (n + N_c e^{-E\beta})}{(\omega)^2 (n + N_c e^{-E\beta})^2 + \omega^2} dE \right] \quad (2.17.2)$$

Pull n from parenthesis,

$$\frac{I_1}{n_1} = \frac{1}{\tau_R} + \omega^2 \nu \sigma \int_0^{E_d} \frac{(M(E) - m_0(E))}{(\nu \sigma n)^2 \left(1 + \frac{N_c}{n} e^{-E\beta}\right)^2 + \omega^2} dE + i\omega \left[1 + \frac{1}{n} \int_0^{E_d} \frac{(M(E) - m_0(E)) \left(1 + \frac{N_c}{n} e^{-E\beta}\right)}{(\nu \sigma n)^2 \left(1 + \frac{N_c}{n} e^{-E\beta}\right)^2 + \omega^2} dE \right] \quad (2.17.3)$$

Now use (2.15) and (2.10) in last equation and divide the imaginary part of the equation (integration part) by $(\nu \sigma n)^2$ to get below equation

$$\frac{I_1}{n_1} = \frac{1}{\tau_R} + \frac{\omega^2 \nu \sigma}{n} \int_0^{E_d} \frac{N_c m_0(E) e^{-E\beta}}{(\nu \sigma n)^2 \left(1 + \frac{N_c}{n} e^{-E\beta}\right)^2 + \omega^2} dE + i\omega \left[1 + \frac{1}{n} \int_0^{E_d} \frac{\left(\frac{N_c}{n} m_0(E) e^{-E\beta}\right) \left(1 + \frac{N_c}{n} e^{-E\beta}\right)}{\frac{\omega^2}{(\nu \sigma n)^2} + \left(1 + \frac{N_c}{n} e^{-E\beta}\right)^2} dE \right] \quad (2.18)$$

Using $n = N_c \exp(-E_{fn}\beta)$ and by defining

$$D = \frac{\omega}{N_c \exp(-E_{fn}\beta)} = \frac{\omega}{n \nu \sigma} \quad (2.19)$$

For simplicity call $\exp(E_{fn} - E)\beta$ as Δ

$$\frac{I_1}{n_1} = \frac{1}{\tau_R} + \omega^2 \nu \sigma \int_0^{E_d} \frac{m_0(E) \Delta}{\omega^2 + (\nu \sigma n)^2 (1 + \Delta)^2} dE + i\omega \left[1 + \frac{1}{n} \int_0^{E_d} \frac{M(E) \Delta}{D^2 + (1 + \Delta)^2} dE \right] \quad (2.20)$$

Try to rewrite (2.20) in terms of $M(E)$ and D by realizing

$$M(E) = m_0(E)(1 + \Delta) \quad (2.20.1)$$

$$D^2 = \left(\frac{\omega}{\nu \sigma n} \right)^2 \quad (2.20.2)$$

$$\frac{I_1}{n_1} = \frac{1}{\tau_R} + \frac{\omega^2}{\nu \sigma n^2} \int_0^{E_d} \frac{M(E)}{D^2 + (1 + \Delta)^2} dE + i\omega \left[1 + \frac{1}{n} \int_0^{E_d} \frac{M(E) \Delta}{D^2 + (1 + \Delta)^2} dE \right] \quad (2.20.3)$$

$$\frac{I_1}{n_1} = \frac{1}{\tau_R} + \int_0^{E_d} \frac{M(E)\Delta D^2 \nu \sigma}{(D^2 + (1+\Delta)^2)(1+\Delta)} dE + i\omega \left[1 + \frac{1}{n} \int_0^{E_d} \frac{M(E)\Delta}{D^2 + (1+\Delta)^2} dE \right] \quad (2.21)$$

Equation (2.21) is in the form $f = A + iB$, now try to simplify the imaginary part of equation(2.21), now consider only the integration part of complex term (B) use (2.19) and rename the required part of (B) as below;

$$G_1(E) = \frac{\omega \Delta}{n(D^2 + (1+\Delta)^2)} = \frac{D \nu \sigma \Delta}{D^2 + (1+\Delta)^2} = \frac{D \nu \sigma \exp\left[\left(E_{fn} - E\right)\beta\right]}{D^2 + \left(1 + \exp\left[\left(E_{fn} - E\right)\beta\right]\right)^2} \quad (2.21.1)$$

Now work with $G_1(E)$, take its derivative with respect to E and equalize the derivative to a zero in order to find the value of D which makes $G_1(E)$ maximum.

$$\frac{dG_1(E)}{dE} = 0 \rightarrow D^2 + 1 = \Delta^2, \text{ for } D \gg 1 \quad D = \Delta \quad (2.22)$$

If we rewrite (2.22) by using definitions used above;

$$D = \Delta \rightarrow \frac{\omega}{N_c \nu \sigma \exp(-E_{fn}\beta)} = \exp\left[\left(E_{fn} - E\right)\beta\right] \rightarrow E_\omega = kTLn\left(\frac{N_c \nu \sigma}{\omega}\right) \quad (2.23)$$

From last part of (2.23) one can rewrite equation for E_ω in order to understand the physical meaning of E_ω ;

$$\omega = N_c \nu \sigma \exp\left(-\frac{E_\omega}{kT}\right); \text{ equation implies that when the thermal emission rate of a}$$

trapped electron at E_ω matches the modulation frequency $G_1(E)$ is maximized. D corresponds to the ratio of emission rates of electrons at that energy level and fermi level.

After notifying the physical meaning of D and E_ω we may continue to work on predefined function $G_1(E)$.

If we plot $G_1(E)$ versus E for roughly guessed values of constants that appear in $G_1(E)$, we see a common behavior (for different E_ω values) of having a sharp peak at $E = E_\omega$ figure 2.1, so one may consider $G_1(E)$ as a multiple of delta function. New form of G is going to be determined through the steps below.

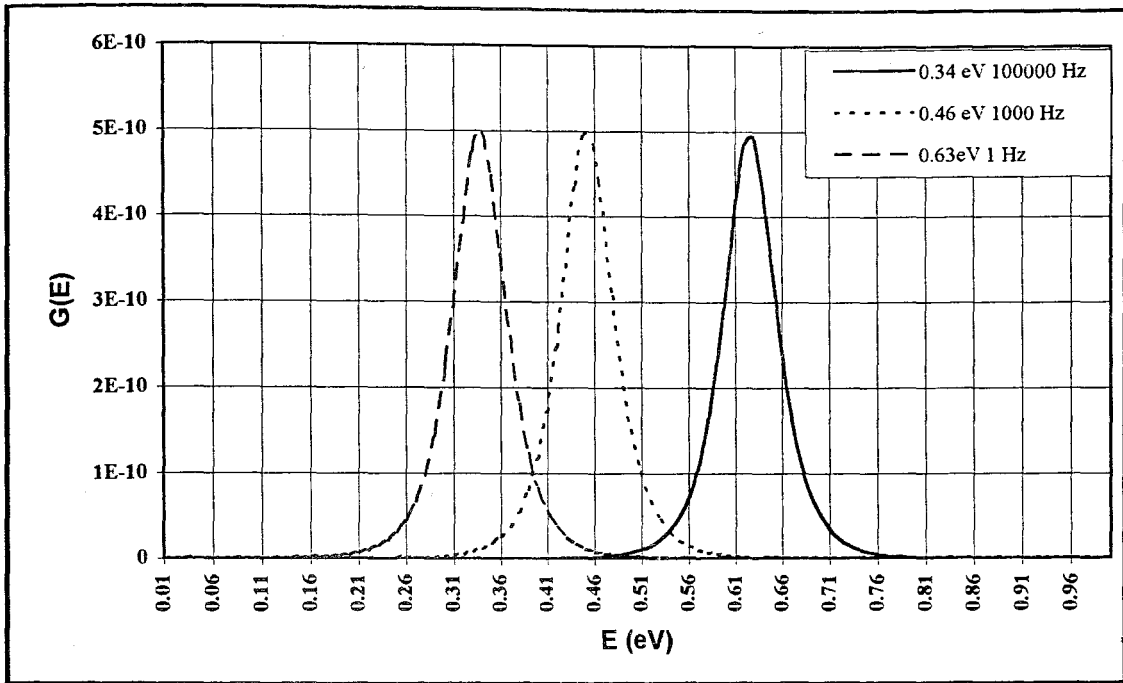


figure 2.2. $G_1(E)$ versus Energy graph

Rewrite $G_1(E)$ by dividing both numerator and denominator by D^2 and using first part of (2.23), one gets;

$$G_1(E) = \frac{\nu\sigma \exp[(E_\omega - E)\beta]}{1 + \left\{ \frac{1}{D} + \exp[(E_\omega - E)\beta] \right\}^2} \quad (2.23.1)$$

And remembering that $D \gg 1$ which cancels $1/D$ term, results with more simpler form for $G_1(E)$, finally;

$$G_1(E) = \frac{\nu\sigma \exp[(E_\omega - E)\beta]}{1 + \exp[2(E_\omega - E)\beta]} \quad (2.24)$$

As mentioned above $G_1(E)$ has also the behavior of delta function, so one may write

$$G_1(E) = J_1 \delta(E - E_\omega) \quad (2.25)$$

It is claimed that last two equations stand for same quantity, so one has to determine the unknown multiplying constant in (2.25) by using this fact.

We are going to use a common trick to determine this constant ,namely integrating both equations (2.24),(2.25) for the interval $(-\infty,\infty)$. Integration of (2.25) is trivial and answer is nothing but the unknown constant itself ,for the integration of (2.24) it is better to start with defining a new variable z ;

$$z = \exp[(E_\omega - E)\beta] \quad (2.25.1)$$

After changing the variable (2.24) turns out to be

$$G_1(E) = \frac{\nu\sigma}{\beta} \int_0^\infty \frac{1}{1+z^2} dz = \frac{\nu\sigma}{2\beta} \int_{-\infty}^\infty \frac{1}{1+z^2} dz = \frac{\nu\sigma}{2\beta} I \quad (2.26)$$

I is also trivial and equals to π so (2.26) or in other words the unknown constant is equal to $\frac{\pi}{2} kT\nu\sigma$. After this step we can rewrite $G_1(E)$ as $\frac{\pi}{2} kT\nu\sigma\delta(E - E_\omega)$

If we put new definition of $G_1(E)$ in (B) we see that the complicated imaginary part becomes;

$$B = \omega + \int_0^{E_d} M(E) \frac{\pi}{2} kT\delta(E - E_\omega) \quad (2.27)$$

If we assume that $M(E)$ varies very slightly around E_ω one may easily evaluate the integral by the help of delta function and the result is ;

$$B = \omega + \frac{\pi}{2} kT\nu\sigma M(E_\omega) \quad (2.28)$$

Now consider the real part of equation (2.21) and rename it as $G_2(E)$, as one may see easily from figure 2.2 $G_2(E)$ has a common behavior for all modulation frequencies of being equal to 1 for the energy values in the interval $(E_\omega < E < E_{jn})$ and being equal to 0 for other energy values. Therefore one may rewrite the real part of equation (2.21) as shown below;

$$A = \frac{1}{\tau_R} + \int_{E_\omega}^{E_{jn}} \nu\sigma M(E) dE \quad (2.28.1)$$

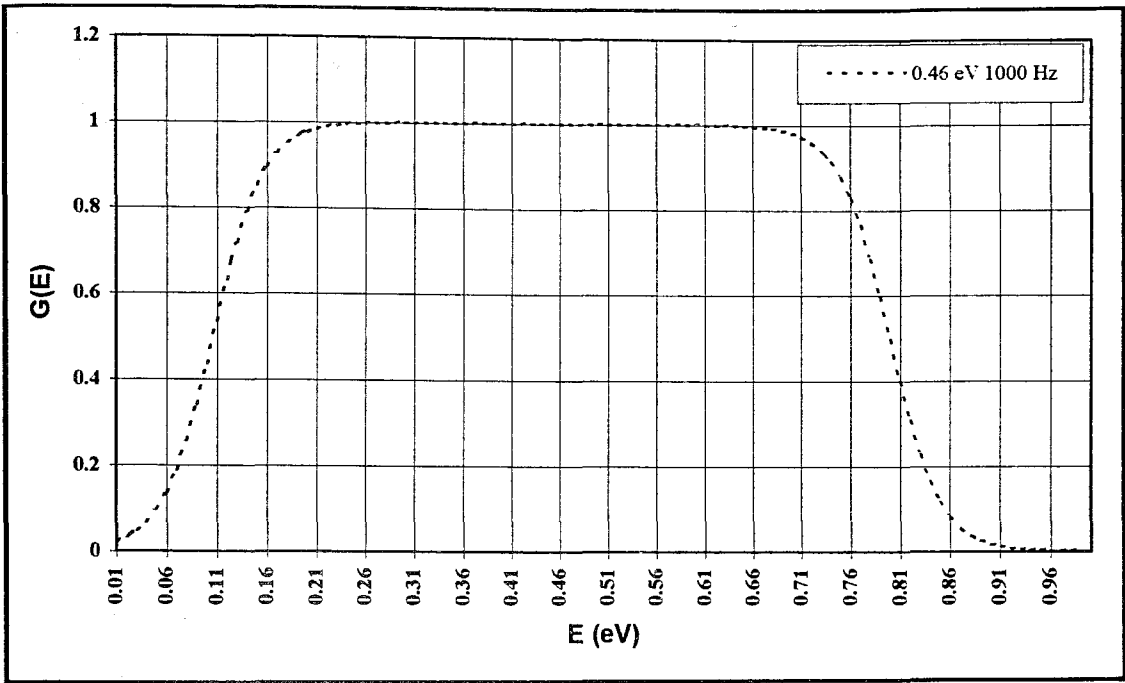


figure 2.3. $G_2(E)$ versus Energy graph.

Now we are going to try to simulate the experiment with these simplified solutions of rate equations, so we have to redefine these equations for experimental purposes.

During the experiment one measures the quantities described below as a function of modulation frequency;

1. photocurrent
2. phase difference between photocurrent and modulating waveform.

Up to here we have the theoretic expression for the rate of carrier generation amplitude and photocurrent amplitude up to a multiplicative constant. The important thing is that this expression is purely defined in terms of $M(E)$ and other material dependent constants. As a measurable quantity none of the above gives this theoretical rate directly but if we look closer to the form of this simplified equation we see that the ratio B/A is directly proportional to the tangent of the phase angle between modulating waveform and photocurrent. One has to notice that modulating waveform and photocurrent -in terms of amplitudes of alternating parts- both directly proportional to I_1 and n_1 respectively and one deduces that phase difference between these quantities -modulating waveform and photocurrent- is exactly the same of those appear on the L.H.S of equation (2.29). In mathematical language;

$$\frac{I_1}{n_1} = A + iB \quad (2.29)$$

$$\tan \phi = \frac{B}{A} = \frac{\omega + \frac{\pi}{2} kT \nu \sigma M(E_\omega)}{\frac{1}{\tau_R} + \int_{E_\omega}^{E_{j_n}} \nu \sigma M(E) dE} \quad (2.30)$$

and ϕ is going to be determined in the experiment.

For experimental purposes real part of the equation (A) has to be redefined because measurements are discrete which implies integral must be a sum and chosen modulation frequency interval may not corresponds to the limits of the integral in equation (2.30). In the experiment one traces an energy interval by changing the modulation frequency and this interval is determined trough the frequency range $(\omega_1 \omega_j)$, so one has to rearrange the border values of equation (2.30) for the appropriate interval.

$$\begin{aligned} E_c \rightarrow E_j \rightarrow \text{trace area} \rightarrow E_1 \rightarrow E_{j_n} \\ \omega_j \rightarrow \dots \rightarrow \omega_1, \quad \omega_1 < \omega_j \end{aligned}$$

If we rewrite denominator of equation (2.30);

$$A = \frac{1}{\tau_R} + \int_{E_1}^{E_{j_n}} \nu \sigma M(E) dE + \int_{E_j}^{E_1} \nu \sigma M(E) dE = \frac{1}{\tau_{R_0}} + \int_{E_j}^{E_1} \nu \sigma M(E) dE \quad (2.31)$$

where

$$\frac{1}{\tau_{R_0}} = \frac{1}{\tau_R} + \int_{E_1}^{E_{j_n}} \nu \sigma M(E) dE \quad (2.32)$$

and in summation form (2.31) turns out to be;

$$A = \frac{1}{\tau_{R_0}} + \sum_{s=2}^j kT \ln \left(\frac{\omega_s}{\omega_{s-1}} \right) \nu \sigma M(E_{s-1}) \quad j = 2, \dots, N \quad (2.33)$$

where $kT \ln \left(\frac{\omega_s}{\omega_{s-1}} \right)$ and N stands for dE and the number of discrete slices - namely number of E_ω and corresponding ω - in the energy interval $(E_j E_1)$ respectively.

Now by using new definitions we can find M(E) from (2.32) and (2.33);

$$\nu \sigma M(E_j) = \frac{2}{\pi kT} \left\{ \left[1 + \sum_{s=2}^j kT \ln \left(\frac{\omega_s}{\omega_{s-1}} \right) \tau_{R_0} \nu \sigma M(E_{s-1}) \right] \tan \phi_j - \omega_j \tau_{R_0} \right\} \quad (2.34)$$

Now consider equation (2.32), $M(E)$ is usually a big number therefore one can neglect the last term in equation (2.34) and one finally gets the equations below;

$$\tau_{R_0} \nu \sigma M(E_1) = \frac{2}{\pi k T} \tan \phi_1 \quad (2.35)$$

$$\tau_{R_0} \nu \sigma M(E_j) = \frac{2}{\pi k T} \left[1 + \sum_{s=2}^j k T \ln \left(\frac{\omega_s}{\omega_{s-1}} \right) \tau_{R_0} \nu \sigma M(E_{s-1}) \right] \tan \phi_j \quad j = 2, \dots, N \quad (2.36)$$

As mentioned above in the experiment one measures the phase difference and a photocurrent as a function of modulation frequency which means we have a extra information to verify the validity of theory. Equation (2.29) enables us to obtain theoretic photocurrent values and compare them with those of obtained during the experiment. If we rewrite equation (2.29) in terms of n_1 we also obtain theoretic expression for photocurrent up to a multiplicative constant.

$$\frac{I_1}{n_1} = A + iB \rightarrow n_1 \propto \frac{1}{\sqrt{A^2 + B^2}} \rightarrow I_{ac} \propto \frac{1}{\sqrt{A^2 + B^2}} \quad (2.37)$$

From (2.37) theoretic expression for photocurrent can be written as;

$$I_{ac}^j = \frac{C}{\left\{ \left[1 + k T \sum_{s=2}^j \ln \left(\frac{\omega_s}{\omega_{s-1}} \right) \tau_{R_0} \nu \sigma M(E_{s-1}) \right]^2 + \left[\pi k T \tau_{R_0} \nu \sigma M(E_j) \right]^2 \right\}^{\frac{1}{2}}} \quad (2.38)$$

It is easy to see that multiplicative constant in equation (2.37) can do no harm ,one can normalize theoretic photocurrent among the set and get rid of the unknown multiplicative constant. After the same normalization procedure applied to a measured photocurrent data set, two sets of values can be compared in order to verify the validity of the theorem.

3. Experimental Method

3.1 Description of the Apparatus

All measurements have been performed using 80386 microprocessor based computer and data acquisition system. This system is supported by the RS232 port and GPIB (General Purpose Interface Adapter) driven by an IEEE 488 board.

For IT (Temperature dependent conductivity measurement) setup KEITHLEY 487 picoammeter and ELIAR temperature controller and for the phase shift measurements 633 nm 5mW laser diode, Model 1681 ITHACO differential amplifier, E&G Model 5110 Dual-phase lock-in amplifier and TES 6102 DC power supply is used.

3.1.1. Temperature dependent conductivity (IT) measurements.

For IT setup as a software support a computer program in Appendix A is used. Program controls 487 Picoammeter via the GPIB and receives the temperature data from temperature controller which uses Platinum resistor (Pt100) as a temperature sensor.

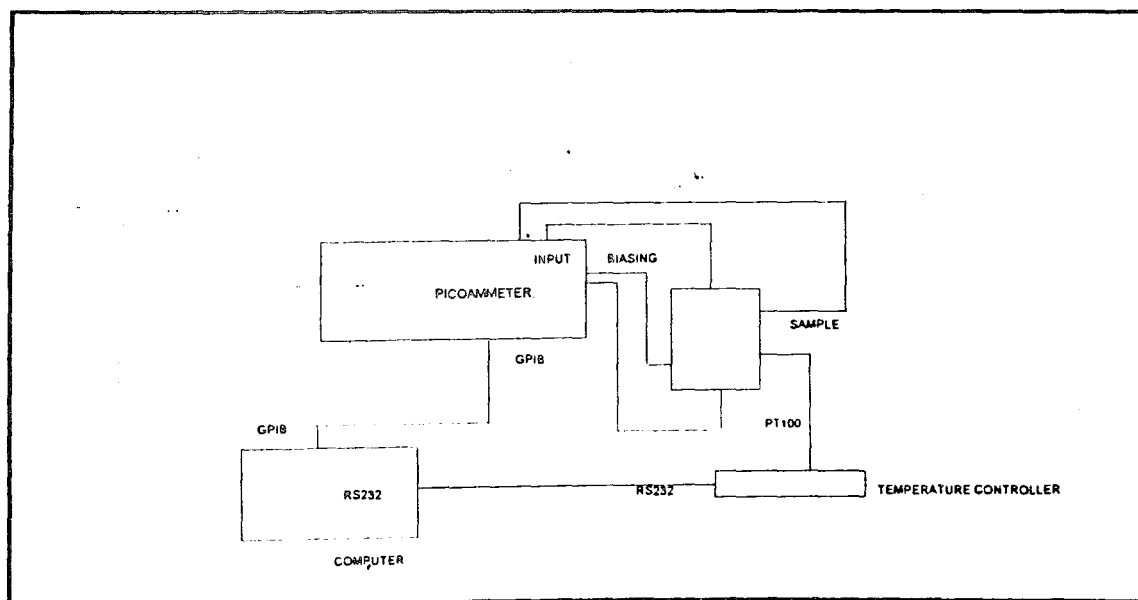


figure 3.1. IT Setup Diagram.

Mainly program requires two parameters to run;

1. The temperature interval to be scanned (T_1, T_2)
2. The step value of the temperature ΔT for interval (T_1, T_2)

The procedure is straightforward, first the sample must be cooled down (or heated) until the required temperature is reached then the program must be run. Program simply records the temperature and current data (for each ΔT eight measurements is taken in a second and average of these data is recorded) at every ΔT in the interval (T_1, T_2) to a file for later processing.

3.1.2 Phase Shift Measurements.

For phase shift measurements the setup in figure 3.2. is used. Lock-in amplifier is remote controlled by computer for lock-in measurements and also as a modulating circuit. The program in Appendix B is used for data recording. Program needs 3 parameters to run;

1. The frequency interval (f_1, f_2)
2. The number of data
3. The type of trace

As mentioned before the lock-in amplifier is used both to determine the frequency-locked measurements and as the modulation driver of the laser diode, the modulation input of the laser diode is directly connected to both modulation output and reference input of lock-in amplifier. The frequency interval (f_1, f_2) can be traced both linearly and logarithmically. The Program provides also a user interface which enables the front panel operations during the data recording process.

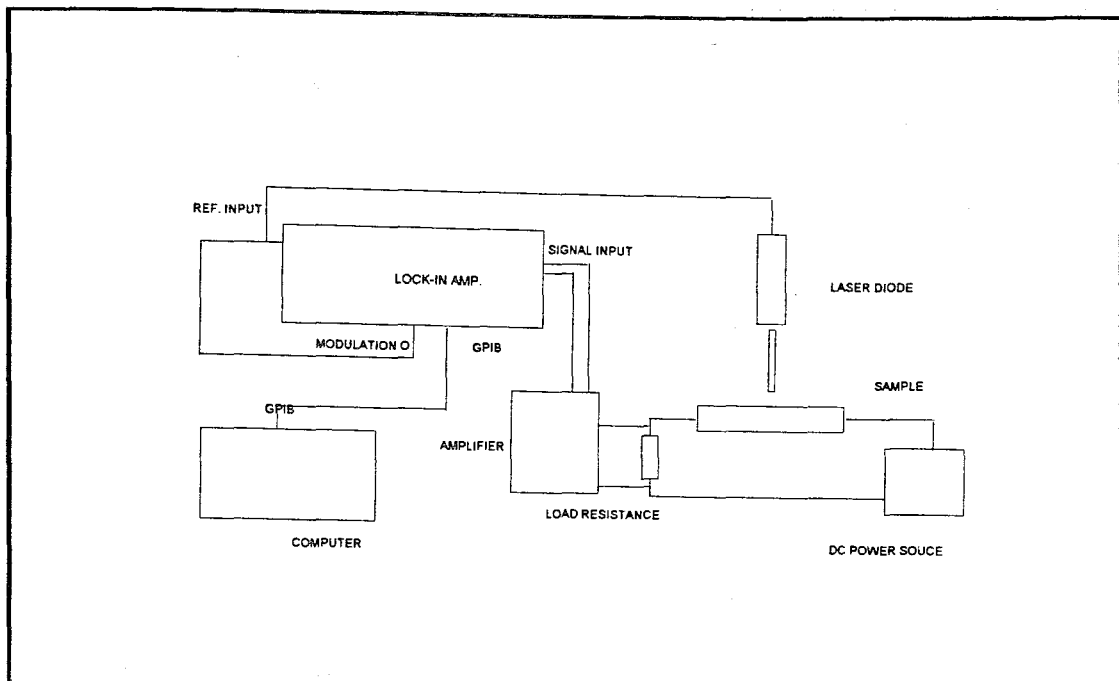


Figure 3.2. Setup diagram for phase-shift measurements.

While the program running computer records 3 parameters independently, these are;

1. The Modulation frequency
2. The Photocurrent
3. The Phase difference between the modulating waveform and the photocurrent

3.2 Results of Measurements.

3.2.1. Initial Procedure.

In the experiment the phase shift between modulating waveform and photocurrent is the basic and the most important parameter and because of the nature of the electronic equipment in the setup one has to be sure that the measured phase difference arises only from the sample.

In order to be sure that this is satisfied firstly modulation output of lock-in amplifier is measured on itself. Namely modulation output is connected to the signal input of lock-in amplifier and for 100 KHz modulation frequency it is observed the phase difference was negligible. Later on phase shift due to modulated laser diode is investigated, for that purpose a nano-second phototransistor is coupled with laser diode. Output signal from biased phototransistor is applied to the signal input of lock-in and the resulted phase shift was again at the order of 0.1 degree at 100 KHz.

Same procedure is repeated with a differential amplifier added to the circuit, this time phase difference at 100 KHz was 4 degree. Therefore for this case whole interval is traced for to obtain phase shift vs. frequency characteristics of differential amplifier.

For a higher value of shunt resistance it is observed that the circuitry cable length also has an extra phase shift effect (via the coupling the capacitance of the cable) and therefore cables is kept short.

After all these, nanosecond phototransistor is replaced with the sample and for different temperatures 20 Hz-100 KHz frequency domain is traced and system's phase shift is than subtracted from each set of data.

3.2.2. Results.

a. IT Measurement Results. Figure 3.4 shows the logarithm of the dark current plotted versus the inverse temperature under constant applied electric field. Activation energy is calculated from the slope of Arrhenius plots taking equation (1.1) as a basis and it is found to be 0.76 eV.

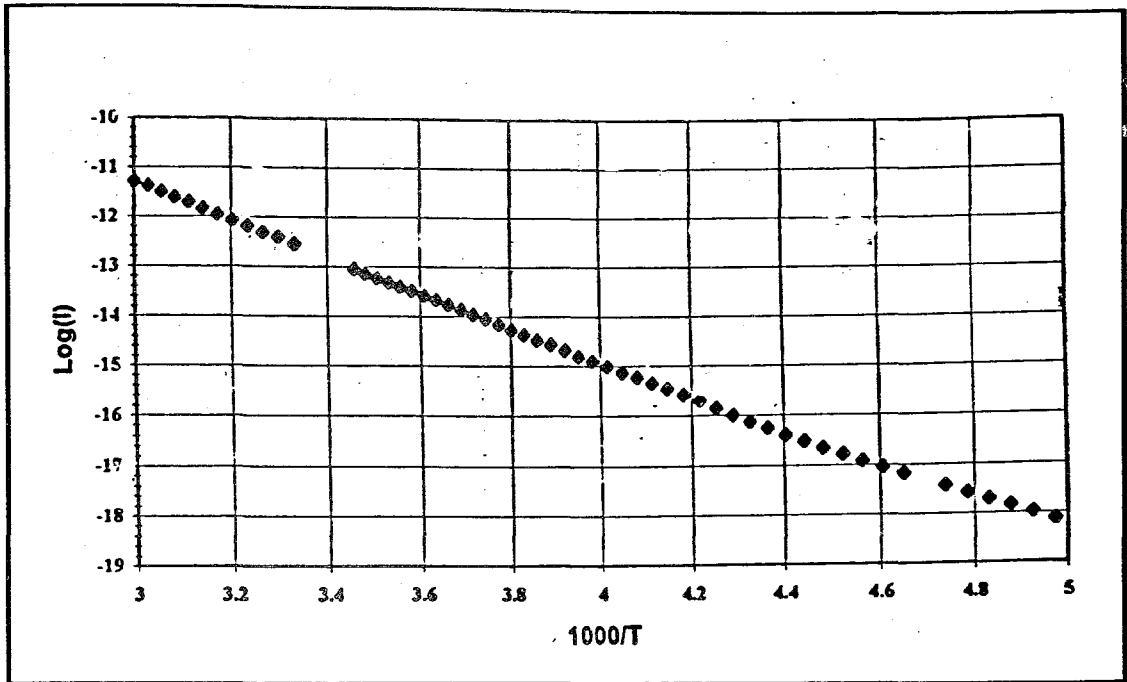


figure 3.3. $\text{Log}(I)$ versus $1000/T$ graph.

b. Phase Shift Measurement Results. For six different temperature values phase shift and intensity is measured as a function of modulation frequency. In each set data, intensity is normalized in order to get normalized experimental photocurrent and this is compared with the theoretical values and from that comparison it is observed that theoretical and experimental values are in perfect agreement. Therefore the validity of theorem is justified.

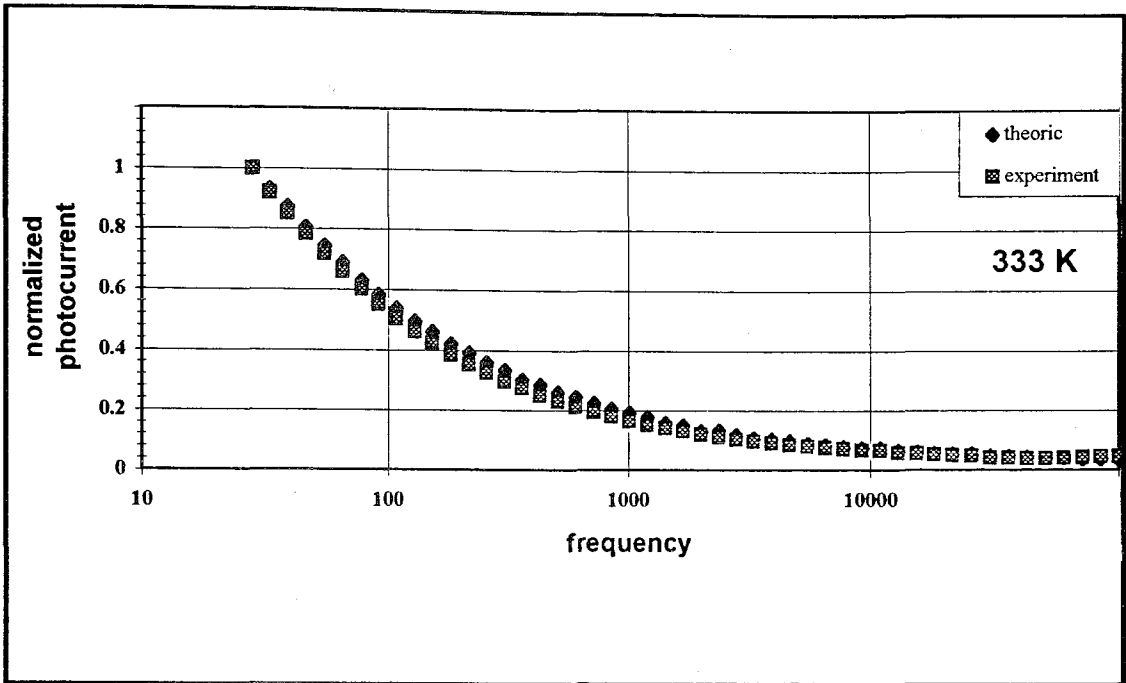


Figure 3.4. Theoretic and experimental photocurrent versus modulation frequency graph for $T=333$ K.

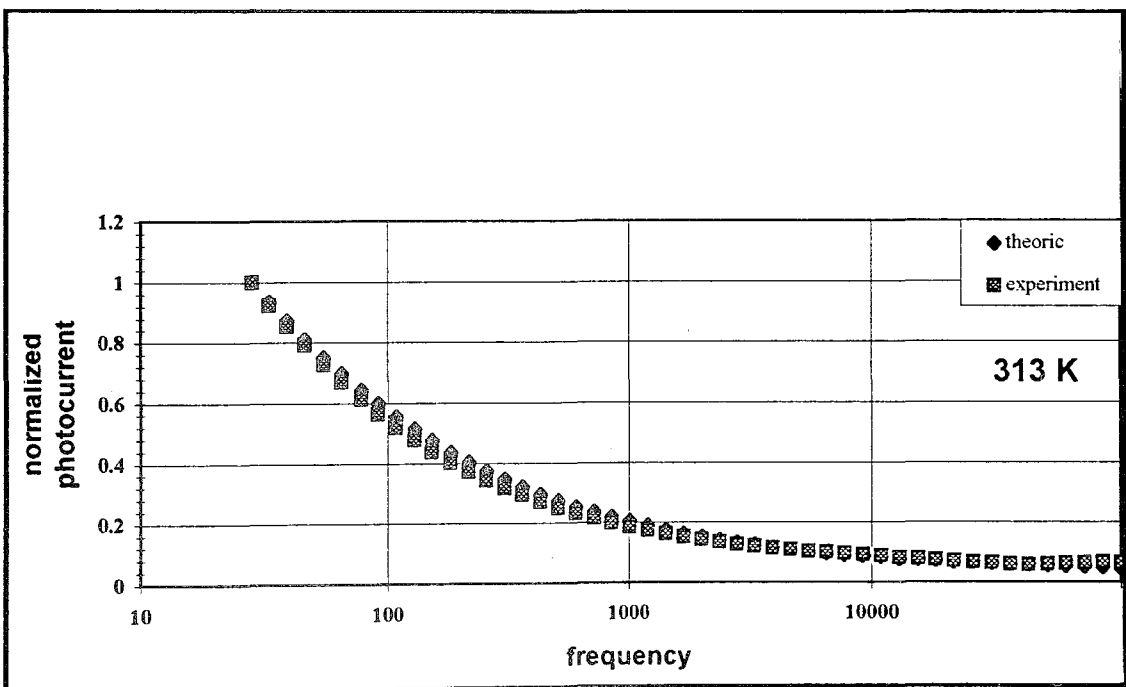


Figure 3.5. Theoretic and experimental photocurrent versus modulation frequency graph for $T=313$ K.

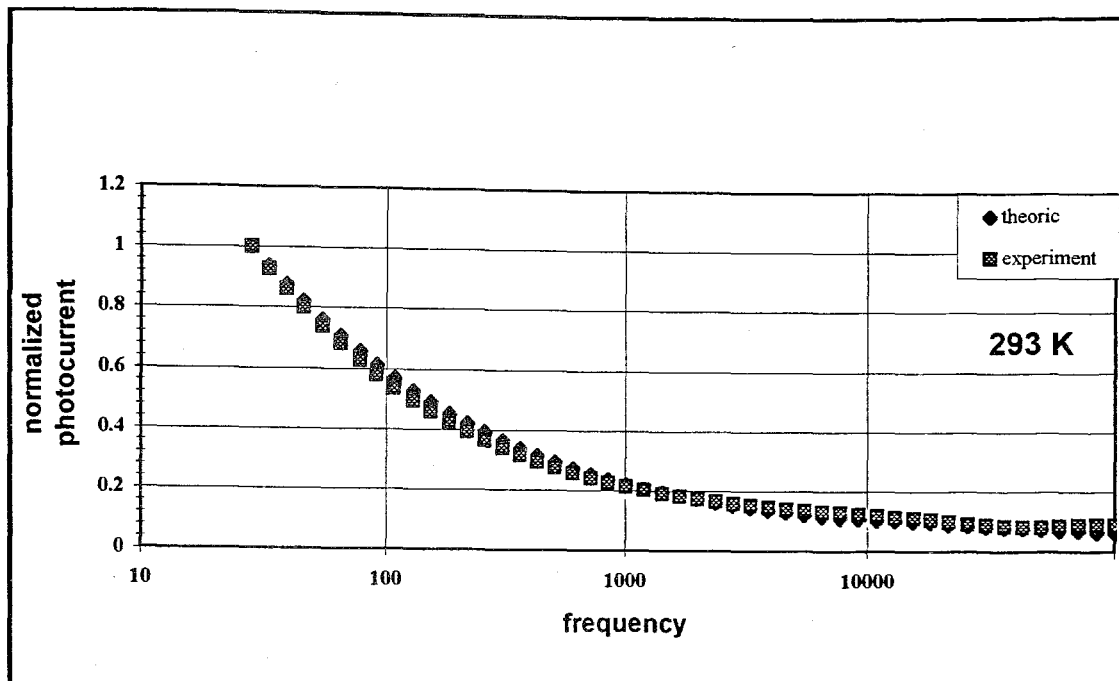


Figure 3.6. Theoretic and experimental photocurrent versus modulation frequency graph for $T=293$ K.

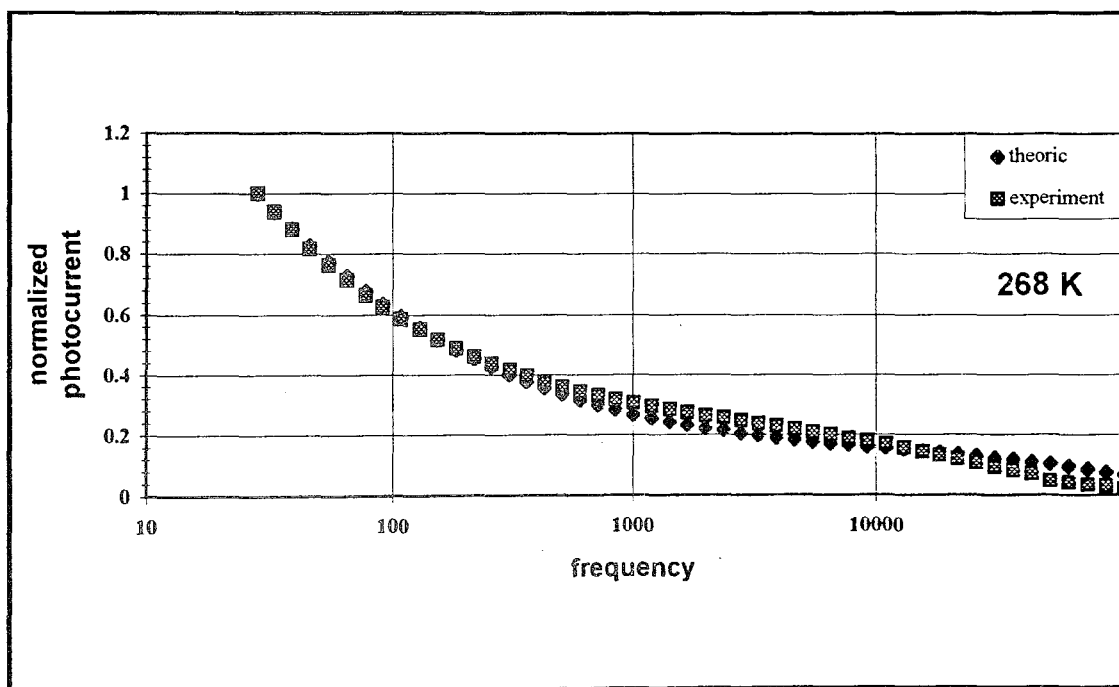


Figure 3.7. Theoretic and experimental photocurrent versus modulation frequency graph for $T=268$ K.

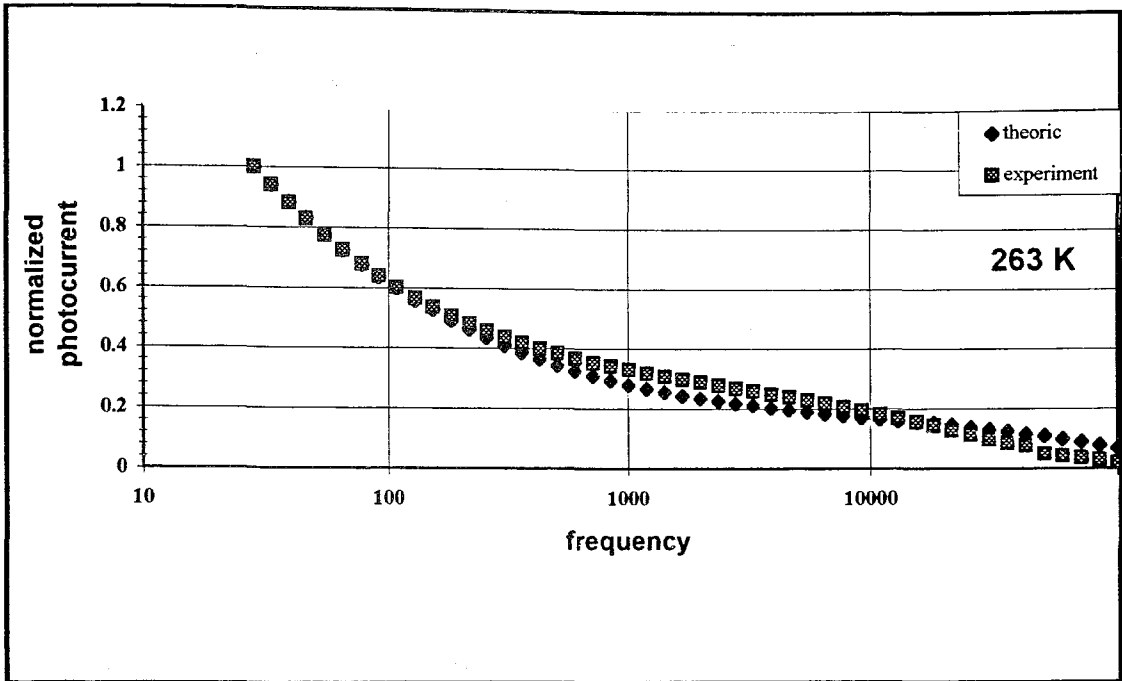


Figure 3.8. Theoretic and experimental photocurrent versus modulation frequency graph for $T=263$ K.

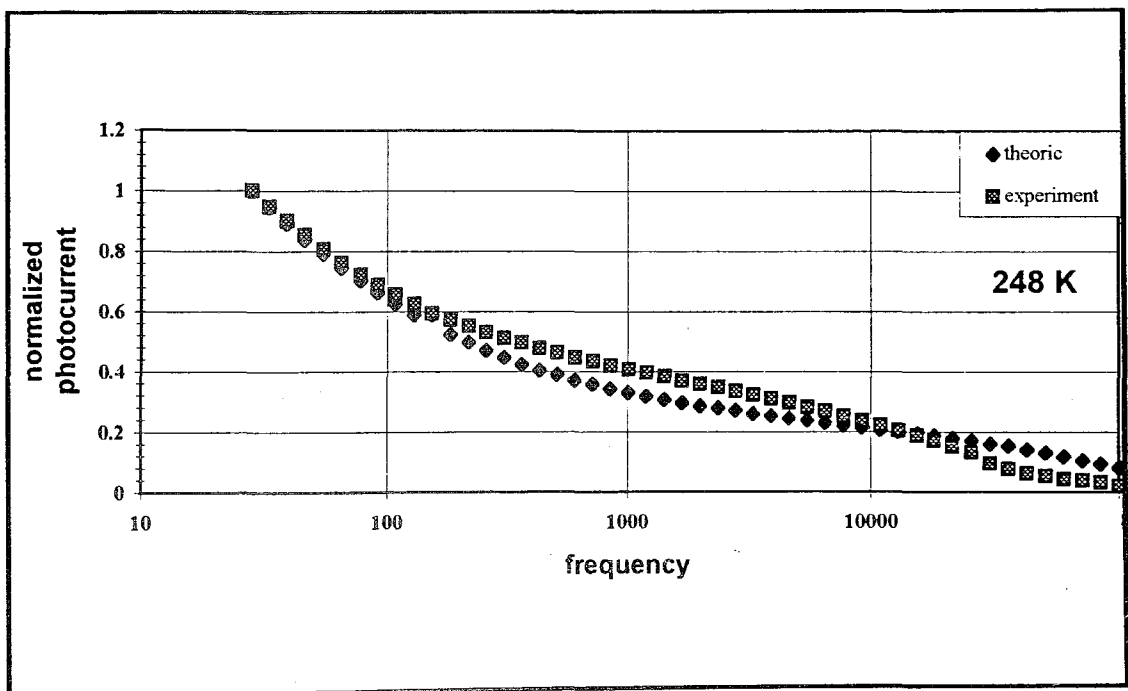


Figure 3.9. Theoretic and experimental photocurrent versus modulation frequency graph for $T=248$ K.

c. The Plot of DOS. The plot of density of states that is $\nu\sigma M(E_j)$ as calculated from equations (2.35) and (2.36) versus the corresponding energy values calculated from (2.23) is shown below.

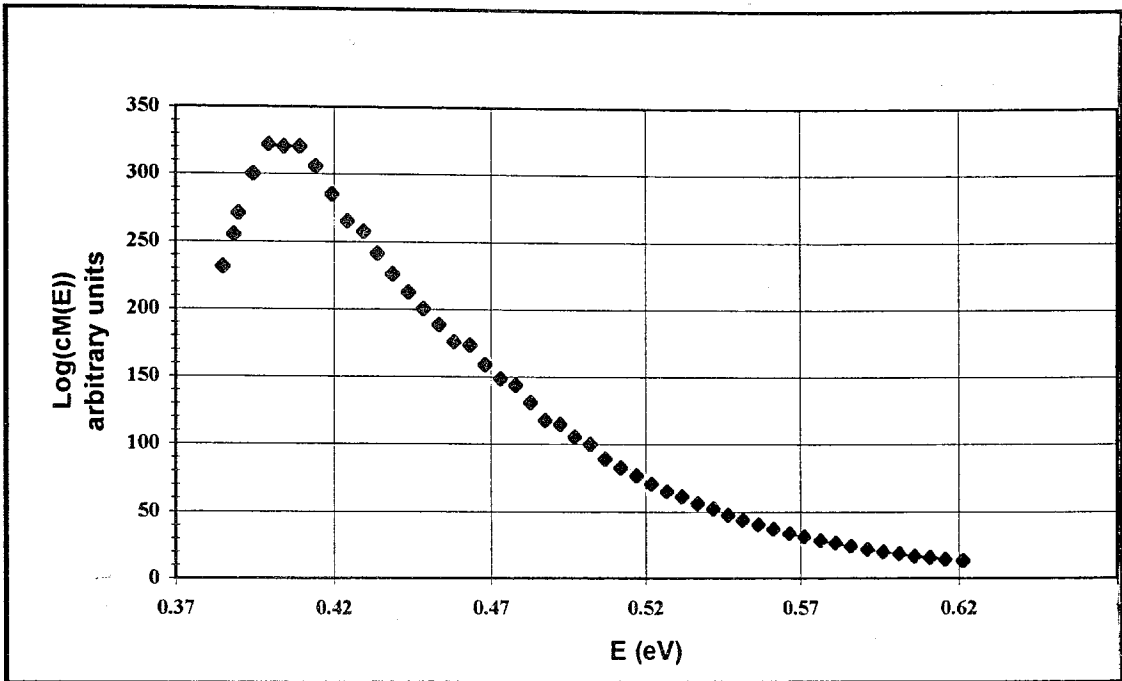


Figure 3.10. The Density of states versus Energy graph, $T=333$ K and $M(E)$ is in arbitrary units.

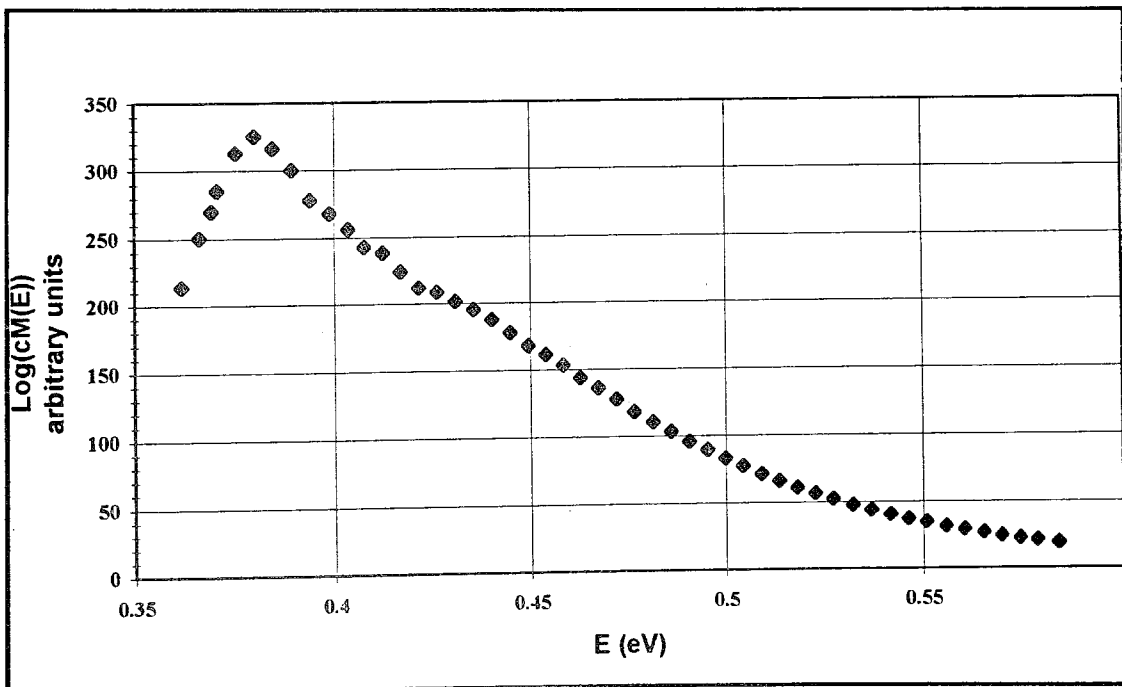


Figure 3.11. The Density of states versus Energy graph, $T=313$ K and $M(E)$ is in arbitrary units.

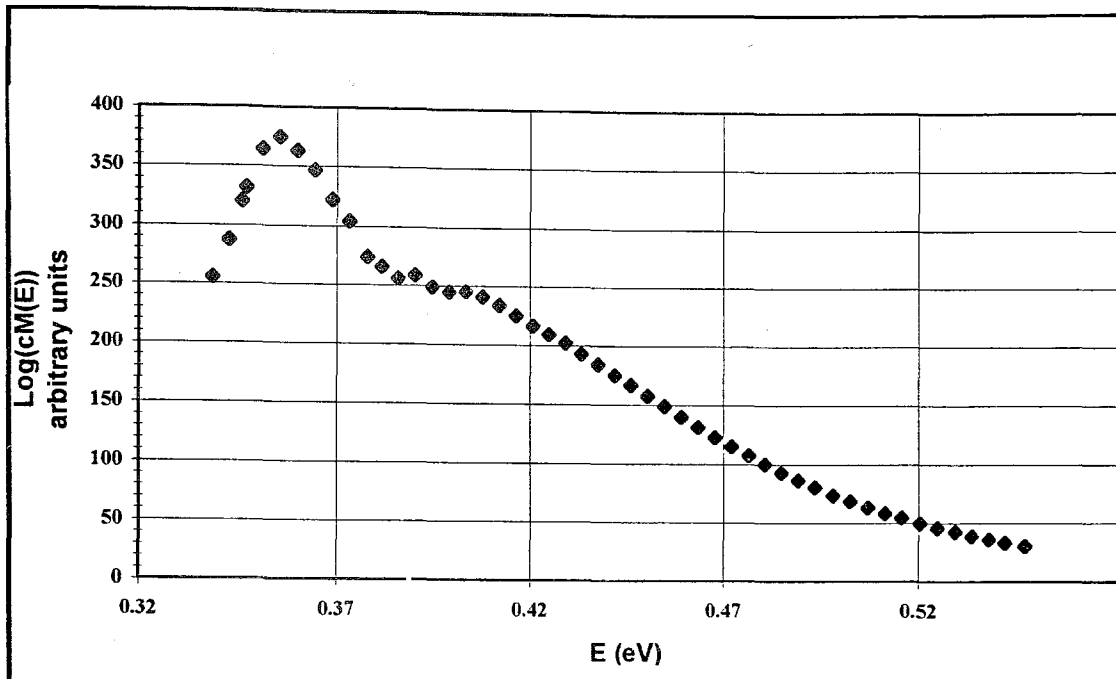


Figure 3.12. The Density of states versus Energy graph, $T=293$ K and $M(E)$ is in arbitrary units.

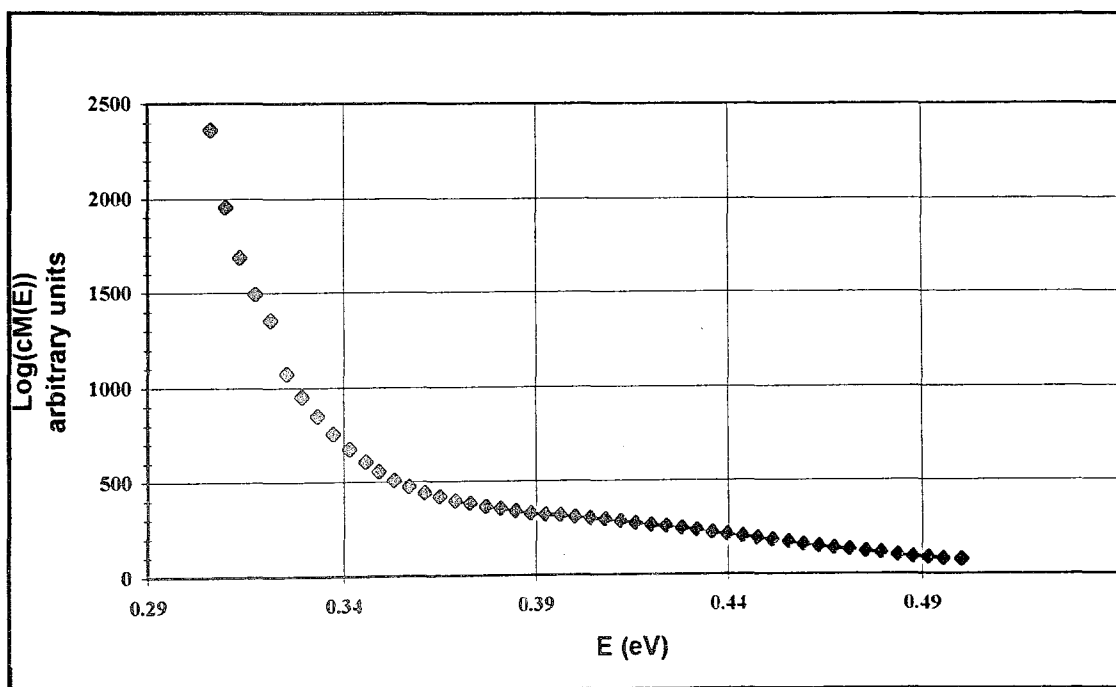


Figure 3.13. The Density of states versus Energy graph, $T=268$ K and $M(E)$ is in arbitrary units.

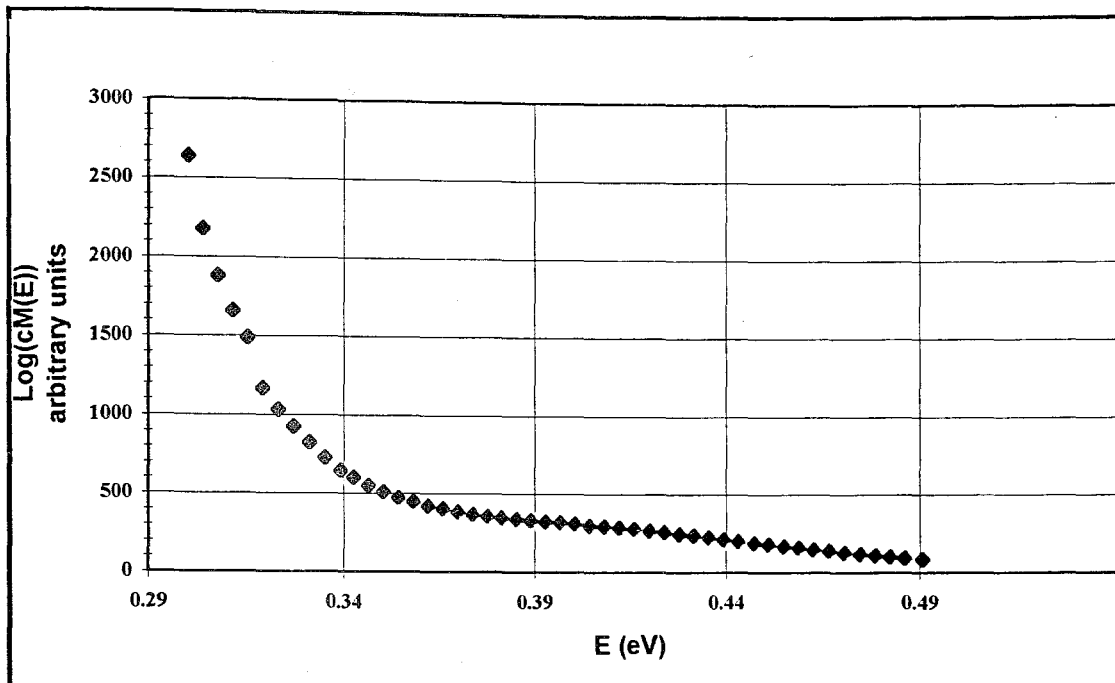


Figure 3.14. The Density of states versus Energy graph, $T=263$ K and $M(E)$ is in arbitrary units.

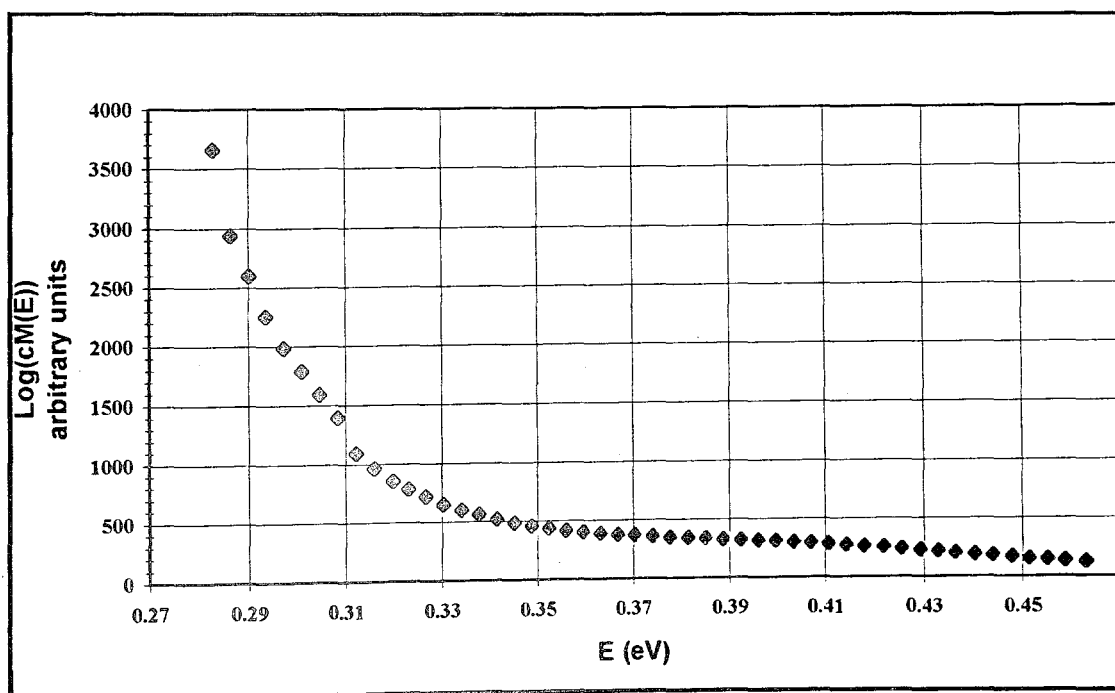


Figure 3.15. The Density of states versus Energy graph, $T=248$ K and $M(E)$ is in arbitrary units.

Within the considered temperature range no shift in energy of the transport path and no thermal activation of the capture cross section is assumed, namely $N_c \nu \sigma$ is kept constant. The narrowing of the optical band gap is ignored thus the shift on the energy axis is due only to the temperature dependence of E_ω and the Figures 3.9. - 3.15. represent partly overlapping sections of same graph.

d. The data process. In order to determine the DOS structure one has to pin each graph into a distinct energy level and one has to consider the missing information due to ambiguity arising from the value of the product $N_c \nu \sigma$.

Now consider Figures Figures 3.9. - 3.15. to determine the overlapping sections one assumes;

$$E(\omega_p, T_p) = E(\omega_q, T_q) \quad (3.1)$$

Therefore one deduces if the equality in equation (3.1) holds from (2.23) one can get

$$\omega_s = N_c \nu \sigma \left(\frac{N_c \nu \sigma}{\omega_{s-1}} \right)^{\frac{-T_{s-1}}{T_s}} \quad (3.2)$$

Equation (3.2) gives ω , T pairs that points the same energy on the axis. If one choose arbitrary ω and repetitively calculates ω , T pairs obtains a set of data for specific energy.

If we plot these pairs ($\ln(\omega)$ vs. $1/T$) from equation (2.23) slope must be the activation energy which is obtained as 0.76 eV. So one can find $N_c \nu \sigma$ by iteration methods as $N_c \nu \sigma = 10^{11}$ from equations (3.2) and (2.23) simultaneously.

Now consider equation (3.1) again which implies;

$$M(E_p) = M(E_q) \quad (3.3)$$

From (2.28) by neglecting ω one obtains;

$$\frac{B_p}{T_p} = \frac{B_q}{T_q} \quad (3.4)$$

and from (2.28.1)

$$A_p = A_q \quad (3.5)$$

One can connect last two equation to get ;

$$\frac{B_p}{A_p T_p} = \frac{B_q}{A_q T_q} \quad (3.6)$$

and from (3.6) and (2.30) one easily obtains;

$$\frac{\tan(\phi_p)}{T_p} = \frac{\tan(\phi_q)}{T_q} \quad (3.7)$$

Now define $\gamma = \frac{\tan(\phi)}{T}$, if one plots γ vs. ω graphs for each set (Figure 3.16), obtained (ω_p, T_p) pairs correspond to same energy.

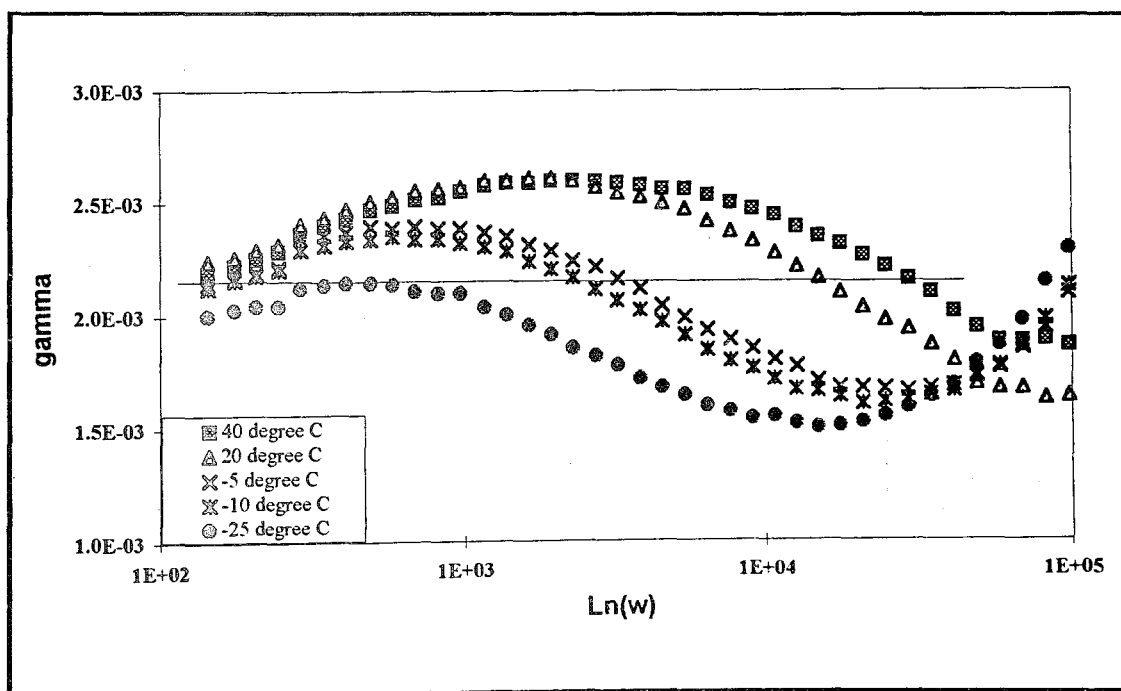


Figure 3.16. Gamma versus frequency graph which determines equal energy (ω, T) pairs. Straight line chooses the corresponding pairs.

Again these same energy pairs can be plotted as in Figure 3.17. from equation (2.23), one obtains $\ln(N_e \nu \sigma)$ as 26.6 graphically which means $N_e \nu \sigma = 10^{11}$ just like before.

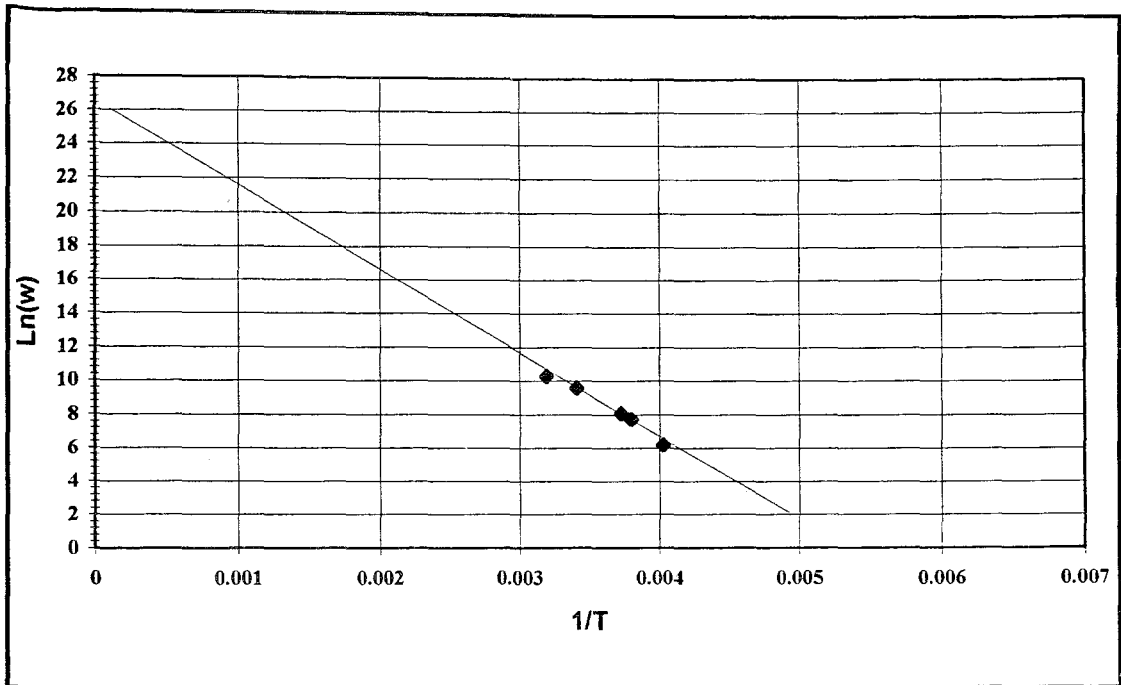


Figure 3.17. ω versus $1/T$ graph, used for to determine $\ln(N_e \nu \sigma)$ graphically.

From this data, frequencies that correspond to same energy can be determined and the required shift on the energy axis performed for each set in a way that all the p pinned to the same location (which can be determined easily via the equation 2.23) on the energy axis. Therefore Figures 3.4. - 3.9. can be replotted together with their correct position on energy axis as Figure 3.18.

Now consider equation (3.5) and $\gamma = \frac{\tan(\phi)}{T}$, define

$$\alpha_j = \frac{\cos(\phi_j)}{I_j} = \frac{A_j}{C_j}, \quad \beta_j = \frac{\sin(\phi_j)}{I_j} = \frac{B_j}{C_j} \quad (3.7)$$

equation (3.5) yields;

$$\frac{C_q}{C_p} = \frac{\alpha_p}{\alpha_q} \quad (3.8)$$

From predetermined pairs one can determine C_n for each set of data via the equation (3.8). C_1 must be chosen arbitrarily. C_n corresponds to the constant that appear on equation (2.38) and the n index stands for the data set number, finally from equation (2.23) one can plot;

$$\nu\sigma M(E_j) = \frac{C_n}{\frac{\pi}{2} kT_n} \beta_j \quad (3.9)$$

The reason that a set dependent constant C_n is introduced is that one has to be sure that the experimental conditions have been kept identical for all the temperatures and C_n guaranties the recovery of systematic inter-set errors. One ensures that each set is properly aligned on $\nu\sigma M(E_j)$ axis. But the selection of first C is arbitrary which scales the $\nu\sigma M(E_j)$ axis, by this method only the relative shift between sets is corrected. Figure 3.18 and Figure 3.19 contains merged and shifted data for the DOS vs Energy;

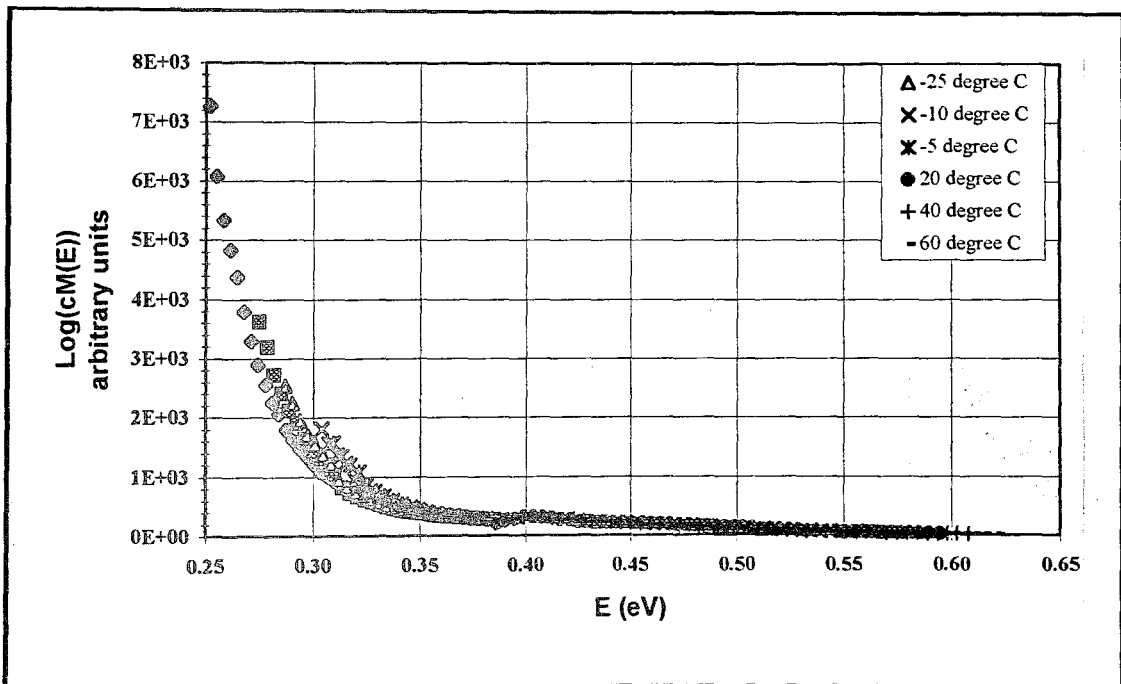


Figure 3.18. DOS versus energy graph.

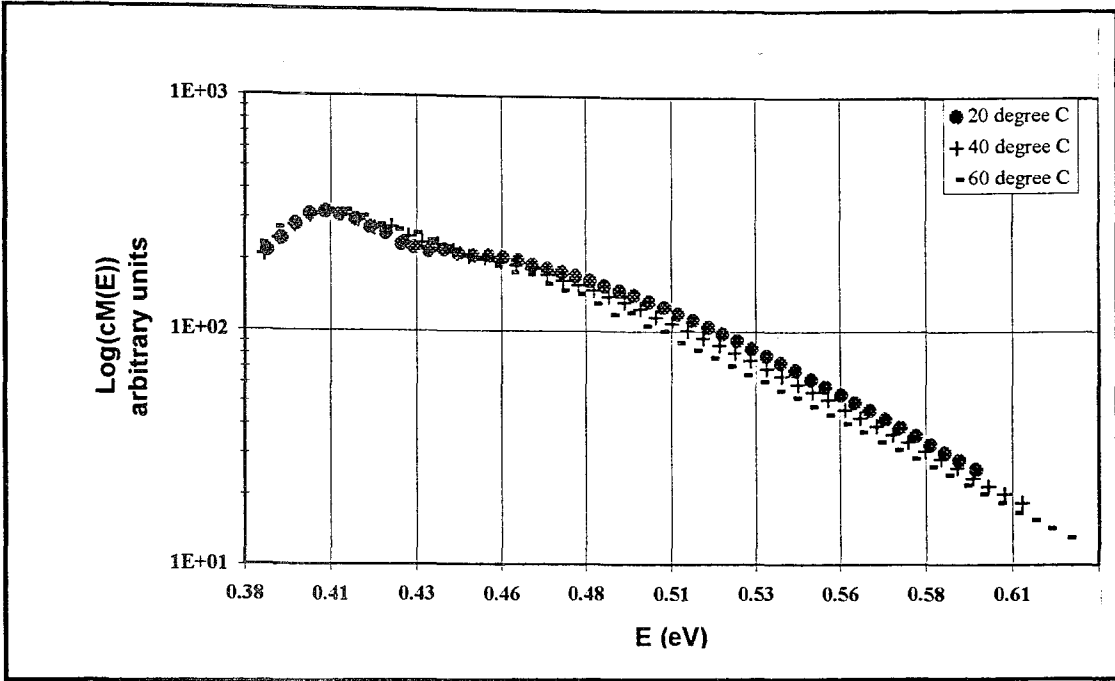


Figure 3.19. DOS versus energy graph.

An absolute determination of the density of states distribution requires an independent measurement of τ_{R_0} , ν , σ otherwise scale can only be given in arbitrary units assuming that σ is not a function of energy.

4. Conclusion

A novel experimental technique for measurements of modulated photocurrents over a wide frequency range has been applied to doped a-Si:H and the phase-shift analysis of modulated photocurrents introduced earlier by Oheda has been revised.

Rate equations are solved for the constrained energy band model, and the solution is expressed in terms of the quantities which are directly related to density of states and the phase shift as the function of modulation frequency. From the experimental data the density of states distribution is obtained for the energy interval about 400 meV. The experimental data yield the DOS distribution above the Fermi level up to about $E_c - 0.25$ eV. Activation energy is determined as 0.76 eV from the IT measurement. CFO type band model (Band tails in the mobility gap) observed as expected. The validity of the theorem is verified by the comparison of theoretic and experimental data, for doped hydrogenated amorphous semiconductor material and the effect of doping is observed at $E_c - 0.40$ eV as a slight deflection from the usual exponential decay behavior.

Some experimental techniques like C-V methods or Field Effect methods have been used for determining the form of these gap states in hydrogenated amorphous silicon. However, there is always possibility of obtaining data about surface states instead of bulk states for this methods but PSAMP method gives the information about DOS only for bulk states because the method requires no MOS (Metal-oxide semiconductor) structure that causes extra surface states trough junctions.

APPENDIX A: COMPUTER PROGRAM USED IN THE I-V MEASUREMENTS

```

'$INCLUDE: 'ieeqb.bi'           'include the file containing
                                'subroutines for IEEE 488 card.

COLOR 14, 9, 3: CLS

DIM ARY1%(600), ARY2%(600)
DIM SHARED D(300) AS INTEGER: LASTCURRENT = 0

PRINT ""
PRINT "This program serves to determine the I-T characteristics"
PRINT "of a given sample by means of the KEITHLEY 487 picoammeter"
PRINT "and ELIAR temperature controller ."
PRINT
PRINT "Turn on the 487 Picoammeter and press any key "
PRINT "to start initialization"

120 A$ = INKEY$
  IF A$ = "" THEN 120

  CALL initialize(21, 0) 'initialize IEEE 488 card

  GOSUB 630 'make zero correction for each range
  GOSUB 880 'open output files
  GOSUB 1010 'ask for the voltage to be applied on the sample
  CALL send(3, "V,1,1X", status%) 'set 487's voltage range to 500 V / 2.5 mA
  s$ = "V" + STR$(VSET) + "X"
  CALL send(3, s$, status%) 'set voltage to the desired value
  CALL send(3, "O1X", status%) 'place V-source in operate mode

PRINT: PRINT "What will be the TEMPERATURE DIFFERENCE between
two"
  INPUT "different measurements (in degrees, 2 or 5 are recommended) ? ",
TSTEP
  TSTEP = CINT(TSTEP)

```

```

t$ = TIMES
time0 = VAL(MID$(t$, 1, 2)) * 3600 + VAL(MID$(t$, 4, 2)) * 60 +
VAL(MID$(t$, 7, 2)) 'start timer for future cooling rate analysis

CLS : GOSUB 500 'read the temperature value sent by ELIAR
260 TARGETTEMP = CINT(TEMPERATURE)
IF TARGETTEMP MOD TSTEP = 0 THEN 300
280 IF TSTEP > 0 THEN TARGETTEMP = TARGETTEMP + 1
IF TSTEP < 0 THEN TARGETTEMP = TARGETTEMP - 1
IF TARGETTEMP MOD TSTEP <> 0 THEN 280 ELSE 310
300 TARGETTEMP = TARGETTEMP + TSTEP
310 PRINT "[ Press (E) to end when necessary , last current read : ";
LASTCURRENT; "]"
PRINT : PRINT "Waiting for "; TARGETTEMP; " degrees"
PRINT : PRINT "The actual temperature is "
340 GOSUB 500 'read the temperature value sent by ELIAR
IF ABS(TEMPERATURE - CINT(TEMPERATURE)) < .15 AND
CINT(TEMPERATURE) = TARGETTEMP THEN CLS : TEMPERATURE =
TARGETTEMP + 273: GOTO 410
LOCATE 5, 27: PRINT USING "+###.#"; TEMPERATURE; : PRINT "
degrees"
IF TSTEP > 0 AND TARGETTEMP < TEMPERATURE THEN CLS :
GOTO 260
IF TSTEP < 0 AND TARGETTEMP > TEMPERATURE THEN CLS :
GOTO 260
IF TSTEP > 0 AND TARGETTEMP - TEMPERATURE > TSTEP * 1.2
THEN CLS : GOTO 260
IF TSTEP < 0 AND TARGETTEMP - TEMPERATURE < TSTEP * 1.2
THEN CLS : GOTO 260

s$ = INKEY$
IF s$ = "E" OR s$ = "e" THEN 1120 'Close and end
GOTO 340
410 'now, measure...
CLS : BEEP: PRINT "Measuring..."

t$ = TIMES

```

```
timeofmsr = VAL(MID$(t$, 1, 2)) * 3600 + VAL(MID$(t$, 4, 2)) * 60 +
VAL(MID$(t$, 7, 2)) ' record the time of this measurement
```

```
meancurrent = 0
```

```
FOR i = 1 TO 50
```

```
CALL send(3, "B0G1X", status%) 'set reading source and data format
```

```
r$ = SPACE$(80): CALL enter(r$, l%, 3, status%): r$ = LEFT$(r$, l%)
```

```
current = VAL(r$)
```

```
meancurrent = meancurrent + current
```

```
NEXT i
```

```
current = meancurrent / 50
```

```
LASTCURRENT = current
```

```
IF timeofmsr < time0 THEN timeofmsr = timeofmsr + 86400 'midnight
correction
```

```
time = timeofmsr - time0 'calculate the time coordinate of the measurement
```

```
' print the results...
```

```
PRINT #1, USING " ##### "; 1000 / TEMPERATURE; : PRINT #1,
USING " +##.### "; LOG(ABS(current)); : PRINT #1, USING " ##### "; time; :
PRINT #1, USING " ### "; TEMPERATURE
```

```
"PRINT #1, 1000 / TEMPERATURE; ", LOG(ABS(CURRENT)); ", 100 /
TEMPERATURE ^ (1 / 4); ", LOG(ABS(CURRENT)); ", TEMPERATURE; ",
CURRENT
```

```
IF FLOPPYFLAG = 1 THEN PRINT #2, USING "### ";
TEMPERATURE; : PRINT #2, USING "+#.#####^"; current; : PRINT #2, USING
" ##### "; time
```

```
CLS : GOTO 300
```

```
' Subroutines used by the main program :
```

```
500 ' Subroutine read the temperature sent by ELIAR through RS-232
```

```
TRIAL = 0
```

```
520 i = 0
```

```

530 IF INP(&H2FD) = 97 THEN i = i + 1: D(i) = INP(&H2F8)
    IF D(i) = 10 THEN 560
    GOTO 530
560 IF TRIAL = 0 THEN TRIAL = 1: GOTO 520
    TEMP$ = CHR$(D(1))
    FOR F = 2 TO 30
    IF D(F) <> 10 THEN TEMP$ = TEMP$ + CHR$(D(F))
    NEXT F
    TEMPERATURE = VAL(TEMP$)
    RETURN

```

630 ' subroutine zero correction for the picoammeter's internal offset currents

```

CLS : PRINT "Please wait..."
WAITINGTIME = 2 'in seconds
CALL send(3, "R1C2X", status%)
CALL send(3, "D WAITX", status%)
GOSUB 1050
CALL send(3, "R2C2X", status%)
CALL send(3, "D WAITX", status%)
GOSUB 1050
CALL send(3, "R3C2X", status%)
CALL send(3, "D WAITX", status%)
GOSUB 1050
CALL send(3, "R4C2X", status%)
CALL send(3, "D WAITX", status%)
GOSUB 1050
CALL send(3, "R5C2X", status%)
CALL send(3, "D WAITX", status%)
GOSUB 1050
CALL send(3, "R6C2X", status%)
CALL send(3, "D WAITX", status%)
GOSUB 1050
CALL send(3, "R7C2X", status%)
CALL send(3, "DX", status%)
CALL send(3, "C0R0X", status%)
RETURN

```

880 ' subroutine open output files

```

CLS : PRINT "Now, if everything is O.K., enter the"
PRINT "output file name ( without [.xls] ) ";
INPUT FILENAMES: PRINT
IF LEN(FILENAMES) > 8 THEN FILENAMES = LEFT$(FILENAMES, 8)
PRINT "Do you want to have a copy of this file "
INPUT "on a floppy disk too ? [y/n] ", FLOPPY$
IF FLOPPY$ = "y" OR FLOPPY$ = "Y" THEN FLOPPYFLAG = 1 ELSE
FLOPPYFLAG = 0
IF FLOPPYFLAG = 1 THEN PRINT : PRINT "Insert a diskette in drive B ":
INPUT "and press ENTER when ready ", OK$
OPEN "A", #1, FILENAMES + ".xls"
IF FLOPPYFLAG = 1 THEN FILENAME2$ = "B:\\" + FILENAMES
IF FLOPPYFLAG = 1 THEN OPEN "A", #2, FILENAME2$
RETURN

1010 ' subroutine input measuring voltage
1020 PRINT : INPUT "Enter the voltage to apply on the sample (in volts) : ",
VSET
IF ABS(VSET) > 501 THEN PRINT : PRINT "Attention": PRINT :
GOTO 1020
PRINT : RETURN

1050 ' subroutine wait during waitingtime
t$ = TIMES$
TIME1 = VAL(MID$(t$, 1, 2)) * 3600 + VAL(MID$(t$, 4, 2)) * 60 +
VAL(MID$(t$, 7, 2))'
1080 A$ = INKEY$
IF A$ = "E" OR A$ = "e" THEN 1120 ELSE t$ = TIMES$
TIME2 = VAL(MID$(t$, 1, 2)) * 3600 + VAL(MID$(t$, 4, 2)) * 60 +
VAL(MID$(t$, 7, 2))'
IF TIME2 - TIME1 < WAITINGTIME THEN 1080 ELSE RETURN

' end of the program...
1120 BEEP: CALL send(3, "C1X", status%): CLOSE : PRINT "The scan is
terminated. Output file name is "; FILENAMES + ".XLS": SYSTEM: END

E N D O F T H E P R O G R A M

```

APPENDIX B: COMPUTER PROGRAM USED IN THE PHASE SHIFT MEASUREMENTS

```

' $INCLUDE: 'c:\programs\ieeeqb.bi'
COLOR 14, 9, 3: CLS
LOCATE 5, 1
PRINT
PRINT "      Note : TURN OFF THE POWER SUPPLY ( AMREL 1326 ) IF
IT IS OPEN,"
PRINT "                                OTHERWISE LOCKIN CANNOT BE REMOTE
CONTROLLED !! "
PRINT
PRINT
PRINT "      Turn on the LOCK-IN AMPLIFIER and press any key "
PRINT "                                to start initialization."
*****INITIALIZATION*****

GOSUB 40000
DEFDBL A, F, I, P, S
DIM ph(200): DIM fr(200): DIM aM(200): DIM i(200): DIM a(200): DIM
sum(200): DIM intensity(200)
FOR z = 0 TO 200: ph(z) = 0: fr(z) = 0: aM(z) = 0: i(z) = 0: a(z) = 0: sum(z) =
0: intensity(z) = 0: NEXT z
m = 21: uni$ = "V": scale = 1: lov = 0: s = 1
T = 300: pi = 3.14159265358979#: kT = T * 8.625E-05: pikT = pi * kT: c1 = 1 /
pikT: rad = pi / 180
CLS : LOCATE 20, 30: PRINT "Initializing...."
CALL initialize(21, 0)
LOCATE 6, 1
25 CLS : GOSUB 12500          'device setup
CLS : GOSUB 12000          'open output files
30 CLS : PRINT "are you going to perform a Logarithmic or Linear trace?"
PRINT "Please answer (L) for logarithmic trace or anything for Linear trace"
INPUT ans$: IF ans$ = "I" OR ans$ = "L" THEN GOTO 50 ELSE GOTO 100

```

50 *****MAIN Logarithmic module*****

CLS : GOSUB 13500 'input and apply measurement freq.

info\$ = "Logarithmic trace mode": ilk = 1: mode = 1

freq = fin: GOSUB 14000

GOSUB 12950

GOSUB 15000: ilk = 0:

lod = 0

55 z\$ = INKEY\$:

IF z\$ = " " THEN GOSUB 15000 'check SPACE for data acceptance

IF z\$ = "+" THEN GOSUB 21000 'increase sensitivity range

IF z\$ = "-" THEN GOSUB 22000 'decrease sensitivity range

IF z\$ = "*" THEN GOSUB 23000 'set offset to zero

IF z\$ = CHR\$(13) THEN GOSUB 24000 'Auto tune single command

IF INT(freq) + st > ffin THEN 200

GOTO 55

100 *****MAIN Linear module*****

CLS : GOSUB 13000 'input and apply measurement freq.

info\$ = "Linear trace mode": ilk = 1: mode = 0

freq = fin: GOSUB 14000

GOSUB 12950

GOSUB 15000: ilk = 0

99 FOR freq = fin TO ffin STEP st

GOSUB 14000 'send!

GOSUB 12950 'check data availability

150 z\$ = INKEY\$:

IF z\$ = " " THEN GOSUB 15000 'check SPACE for data acceptance

IF z\$ = "+" THEN GOSUB 21000 'increase sensitivity range

IF z\$ = "-" THEN GOSUB 22000 'decrease sensitivity range

IF z\$ = "*" THEN GOSUB 23000 'set offset to zero

IF z\$ = CHR\$(13) THEN GOSUB 24000 'Auto tune single command

IF INT(freq) + st > ffin THEN 200

GOTO 150

200 LOCATE 21, 1

BEEP: CLOSE : PRINT TAB(16); "Scan is terminated. Output file name is ";

FILENAMES

```
PRINT : PRINT TAB(11); "Do you want to perform another scan on this sample
(Y/N) ? "
```

```
210 a$ = INKEY$
```

```
IF a$ = "" THEN 210
```

```
IF a$ = "y" OR a$ = "Y" THEN CLS : GOTO 25
```

```
END
```

```
12000 '*****subroutine (open output files)*****
```

```
LOCATE 5, 20
```

```
PRINT "Now, if everything is O.K., enter the"
```

```
LOCATE 6, 20: PRINT "output file name (without extension) "
```

```
PRINT TAB(30); : INPUT FILENAMES$: PRINT : PRINT
```

```
IF LEN(FILENAMES) > 8 THEN FILENAMES$ = LEFT$(FILENAMES$, 8)
```

```
PRINT TAB(20); "Do you want to have a copy of this file "
```

```
PRINT TAB(20); : INPUT "on a floppy disk too ? [y/n] ", FLOPPY$
```

```
IF FLOPPY$ = "y" OR FLOPPY$ = "Y" THEN FLOPPYFLAG = 1 ELSE
FLOPPYFLAG = 0
```

```
IF FLOPPYFLAG = 1 THEN PRINT : PRINT : PRINT TAB(24); "Insert a
diskette in drive B ": PRINT TAB(25); : INPUT "and press ENTER when ready ", OK$
```

```
FILENAMES$ = FILENAMES$ + ".xls"
```

```
OPEN "A", #1, FILENAMES$
```

```
IF FLOPPYFLAG = 1 THEN FILENAME2$ = "B:\\" + FILENAMES$
```

```
IF FLOPPYFLAG = 1 THEN OPEN "A", #2, FILENAME2$
```

```
RETURN
```

```
12500 '*****subroutine (device setup)*****
```

```
disp1$ = "D1 1"
```

```
disp2$ = "D2 2"
```

```
phase$ = "P 0 0"
```

```
oa$ = "oa 5000"
```

```
CALL send(5, disp1$, status%)
```

```
CALL send(5, disp2$, status%)
```

```
CALL send(5, phase$, status%)
```

```
CALL send(5, oa$, status%)
```

```
RETURN
```

```

12950 '*****subroutine(data available?)*****
      FRQ$ = "FRQ"
      CALL send(5, FRQ$, status%)
      f$ = SPACES(80): CALL enter(f$, L%, 5, status%)
      f$ = LEFT$(f$, L%)
      fcon = VAL(f$) * .001:
      IF (ABS((fcon - freq) / freq) <= .02) THEN RETURN
      GOTO 12950
13000 '****subroutine (input and apply measurement frequency linear)****
      CLS
13010
      PRINT "Enter the initial FREQUENCY (smaller one!) (in Hertz) "
      PRINT : INPUT fin
      IF fin < .5 OR fin > 100000 THEN PRINT : PRINT : PRINT TAB(35); "A t t
e n t i o n !": PRINT : PRINT TAB(15); "The frequency should be in the range 0.5 Hz -
1 kHz...": PRINT : GOTO 13010
13020
      CLS
      PRINT "Enter the final FREQUENCY (in Hertz) "
      PRINT : INPUT ffin
      IF ffin < .5 OR ffin > 100000 THEN PRINT : PRINT : PRINT TAB(35); "A t t e
n t i o n !": PRINT : PRINT TAB(15); "The frequency should be in the range 0.5 Hz - 1
kHz...": PRINT : GOTO 13020
13030
      CLS
      PRINT "Enter the STEP FREQUENCY (in Hertz) "
      PRINT : INPUT st
      CLS
      PRINT "Linear increase will be executed"
      PRINT "start frequency is "; fin; " Hz"
      PRINT "stop frequency is "; ffin; " Hz"
      PRINT "step frequency is "; st; " Hz"
      PRINT : PRINT TAB(11); "Do you want to change the values (Y/N) ? "
13035
      a$ = INKEY$
      IF a$ = "" THEN 13035
      IF a$ = "y" OR a$ = "Y" THEN CLS : GOTO 30
      CLS

```

RETURN

13500 '****subroutine (input and apply measurement frequency logarithmic)****

CLS

13510

PRINT "Enter the initial FREQUENCY (smaller one!) (in Hertz) "

PRINT : INPUT fin

IF fin < .5 OR fin > 100000 THEN PRINT : PRINT : PRINT TAB(35); "A t t e
n t i o n !": PRINT : PRINT TAB(15); "The frequency should be in the range 0.5 Hz - 1
kHz...": PRINT : GOTO 13010

13520

CLS

PRINT "Enter the final FREQUENCY (in Hertz) "

PRINT : INPUT ffin

IF ffin < .5 OR ffin > 100000 THEN PRINT : PRINT : PRINT TAB(35); "A t t e
n t i o n !": PRINT : PRINT TAB(15); "The frequency should be in the range 0.5 Hz - 1
kHz...": PRINT : GOTO 13020

13530

CLS

PRINT "Enter the number of measurements in that interval "

PRINT : INPUT stl

CLS

PRINT "Logarithmic increase will be executed"

PRINT "start frequency is "; fin; " Hz"

PRINT "stop frequency is "; ffin; " Hz"

PRINT "number of data in that interval is"; stl

logfreq = LOG(fin) / LOG(10)

PRINT : PRINT TAB(11); "Do you want to change the values (Y/N) ? "

13535

a\$ = INKEY\$

IF a\$ = "" THEN 13535

IF a\$ = "y" OR a\$ = "Y" THEN CLS : GOTO 30

CLS

RETURN

```

14000 '*****subroutine (frequency range calculation, sending!)*****
      IF freq < 2 AND freq >= .5 THEN N = 0
      IF freq < 20 AND freq >= 1.8 THEN N = 1
      IF freq < 200 AND freq >= 18 THEN N = 2
      IF freq < 2000 AND freq >= 180 THEN N = 3
      IF freq < 20000 AND freq >= 1800 THEN N = 4
      IF freq < 105000 AND freq >= 18000 THEN N = 5
      fconvtd = freq * 10 ^ (4 - N): fconvtd = INT(fconvtd)
      frequency$ = "OF" + STR$(fconvtd) + STR$(N)
      CALL send(5, frequency$, status%)
      RETURN

15000 '*****subroutine (receiving data from lockin)*****
      FRQ$ = "FRQ"
      pha$ = "PHA"
      mag$ = "mag"
      CALL send(5, FRQ$, status%)
      f$ = SPACES$(80): CALL enter(f$, L%, 5, status%)
      f$ = LEFT$(f$, L%)
      CALL send(5, pha$, status%)
      p$ = SPACES$(80): CALL enter(p$, L%, 5, status%)
      p$ = LEFT$(p$, L%)
      CALL send(5, mag$, status%)
      m$ = SPACES$(80): CALL enter(m$, L%, 5, status%)
      m$ = LEFT$(m$, L%)
      ma = VAL(m$)
      magn = (ma / 10000) * scale
      IF uni$ = "V" THEN inten = magn
      IF uni$ = "mV" THEN inten = magn * 10 ^ -3
      IF uni$ = "uV" THEN inten = magn * 10 ^ -6
      IF uni$ = "nV" THEN inten = magn * 10 ^ -9
      GOSUB 18000:
      IF mode = 1 THEN GOSUB 35000
      NEXT freq
      RETURN

```

```

18000 ***** subroutine (print the results) *****
      CLS :
      LOCATE 8, 1: PRINT info$: PRINT : PRINT "range is"; STR$(scale) + uni$:
PRINT
      IF lov = 0 THEN lov$ = "auto offset operation not executed yet" ELSE lov$ =
"Last AXO operation executed at " + STR$(lastfreq) + "Hz"
      PRINT lov$
      LOCATE 1, 13: PRINT "KEY COMMANDS": PRINT
      PRINT "+.....increases sensitivity range"
      PRINT "-.....decreases sensitivity range"
      PRINT "*.....sets offset to zero      "
      PRINT "enter...performs single autotune  "
      LOCATE 16, 1: PRINT "LAST READ"
      PRINT " f(hz) = "; : PRINT USING "#####.###"; fcon; : PRINT ; "
phase(dgr) ="; : PRINT USING "+###.###"; VAL(p$) * .001
      PRINT "voltage ="; : PRINT USING "###.###"; magn; : PRINT " "; uni$; :
PRINT " or ="; : PRINT USING "#.#####"; inten; : PRINT " volts"
      IF ilk = 1 THEN RETURN
      LOCATE 13, 1: PRINT "calculating"
      IF s > 1 THEN GOTO 19000
      ph(1) = ABS(VAL(p$) * .001 * rad)
      fr(1) = VAL(f$) * .001
      aM(1) = c1 * TAN(ph(1)):
      i(1) = 1
      intensity(1) = inten: IF s = 1 THEN GOTO 20000

19000 ph(s) = ABS(VAL(p$) * .001 * rad)
      fr(s) = VAL(f$) * .001
      intensity(s) = inten
      a(s) = kT * LOG((fr(s) / fr(s - 1))) * aM(s - 1)
      sum(s) = sum(s - 1) + a(s)
      aM(s) = c1 * (1 + sum(s)) * TAN(ph(s))
      i(s) = SQR((1 + (TAN(ph(1))) ^ 2)) / SQR(((1 + sum(s)) ^ 2 + (pikT * aM(s)) ^
2))

20000 PRINT #1, USING "#####.###"; fr(s); : PRINT #1, ","; : PRINT #1,
USING "+###.###"; VAL(p$) * .001; : PRINT #1, ","; : PRINT #1, USING "
###.#####"; intensity(s); : PRINT #1, ",";

```

```

PRINT #1, USING "####.#####"; i(s); : PRINT #1, ", "; : PRINT #1, USING "
###.#####"; aM(s)
s = s + 1
RETURN
21000 '*****subroutine that increases sensitivity range*****
m = m + 1: IF m = 22 THEN m = 21
sen$ = "SEN" + STR$(m)
CALL send(5, sen$, status%)
GOSUB 22500
RETURN
22000 '*****subroutine (decreases sensitivity range)*****
m = m - 1: IF m = -1 THEN m = 0
sen$ = "SEN" + STR$(m)
CALL send(5, sen$, status%)
GOSUB 22500
RETURN
22500 '*****subroutine (determines sensitivity)*****
IF (m - 0) / 3 = INT((m - 0) / 3) THEN taban = 1
IF (m - 1) / 3 = INT((m - 1) / 3) THEN taban = 2
IF (m - 2) / 3 = INT((m - 2) / 3) THEN taban = 5
power = INT(m / 3) - 7
IF m = 21 THEN uni$ = "V"
IF m < 21 AND m > 11 THEN uni$ = "mV"
IF m < 12 AND m > 2 THEN uni$ = "uV"
IF m < 3 THEN uni$ = "nV"
IF uni$ = "V" THEN scale = 1
IF uni$ = "mV" THEN scale = taban * 10 ^ (3 - ABS(power))
IF uni$ = "uV" THEN scale = taban * 10 ^ (6 - ABS(power))
IF uni$ = "nV" THEN scale = taban * 10 ^ (9 - ABS(power))
RETURN
23000 '*****subroutine (sets ofset to zero)*****
axo$ = "axo"
CALL send(5, axo$, status%)
lastfreq = VAL(f$) * .001
lov = 1
RETURN

```

```
24000 '*****subroutine (perform auto single tune)*****
    AT$$ = "ats"
    CALL send(5, AT$$, status%)
    RETURN
30000 '*****subroutine (calculates logarithmic steps)*****
    logst = (LOG(ffin / fin)) / ((stl) * LOG(10))
    logfreq = logfreq + logst
    freq = 10 ^ logfreq
    freq = INT(freq)
    IF freq > ffin THEN 200
    RETURN
35000 '*****subroutine (decides that log loop is okay)*****
    GOSUB 30000
    GOSUB 14000
    GOSUB 12950
    IF freq > ffin THEN 200
    RETURN

40000
    a$ = INKEY$
    IF a$ = "" THEN 40000
    RETURN
'E N D   O F   P R O G R A M'
```

REFERENCES

- [1] Chittick R.C., Alexander J.H. and Sterling H.F., *Journal of Electrochem. Soc.* Vol. 116, No. 77, 1969.
- [2] Chittick R.C., *Journal of Non-Crystalline Solids* Vol. 3, No. 255, 1970.
- [3] Adler D., *Proceedings of the Kyoto Summer Institute*, "Defects in Covalent Amorphous Semiconductors", ed. Yonezawa F., (Springer-Verlag, Berlin, 1981).
- [4] Brodsky M.H. and Gambino R.J., *Journal of Non-Crystalline Solids*, Vol. 8, No. 10, 1972.
- [5] Çaglayan B., M.S. thesis, Bogaziçi University, 1982.
- [6] Dellafera P., Labush R. and Roscher H.H., *Phil. Mag.* Vol. B 43, No. 1, 1981.
- [7] Oheda H., *Journal of Appl. Phys.*, Vol. 52, No. 11, 1981.
- [8] Brodsky M.H., Title R.S., Weiser K., Pettit G.D., *Phys. Rev.* Vol. B 1, pp. 2632-2636, 1970.
- [9] Adler D., *Phys. Rev. Lett.* Vol. 41, pp. 1755-1760, 1978.
- [10] Brodsky M.H., Cuomo J.J., *Amorphous and Liquid Semiconductors*, ed. by Spear W.E. (University of Edinburgh, Edinburgh, 1977), 1924.
- [11] Spear W.E., *Amorphous and Liquid Semiconductors* ed. by Stuke J. and Brenig W. (Taylor and Francis, London, 1975)
- [12] Moustakas T.D., Anderson D.A., Poul W., *Solid state commun.* Vol. 23, No. 43, 1980, I. Solomon, Perrin J., Bourdon B., *Inst. Phys. Conf. Ser.* Vol. 43, No. 689 1979.
- [13] Tauc J., *Amorphous and Liquid Semiconductors*, ed. by Touc J. (Plenum, New York, 1974), Ch. 4.
- [14] Anderson D. A., Spear W.E., *Phil. Mag.* Vol. 36, pp. 695-701, 1977.
- [15] Spear W.E., Lecomber P.G., *Phil. Mag.* Vol. 33, pp. 935-949, 1976.
- [16] Spear W.E., Lecomber P.G., *Topics in Appl. Phys.* Vol. 36 pp. 251-255, 1979.
- [17] Spear W.E., Lecomber P.G., *Solid State Commun.* Vol. 17 pp. 1193-1196, 1975.
- [18] Spear W.E., Lecomber P.G., Madan A., *J. Non-Cryst. Solids*, Vol. 11 pp. 219-221, 1972
- [19] Lewis A.J., Connel G.A.N., Paul W., Pawlik J.R., Temkin R.J., *Tetrahedrally Bonded Amorphous Semiconductors*, ed. by Brodsky M., Kirkpatrick S., Weaire D. (American Institute of Physics, New York 1974), pp. 27-32.
- [20] Lewis A.J., *Phys. Rev.* Vol. B, No. 14 pp. 658-665, 1976.

- [21] Paul W., Pawlik J.R., *Proceedings of the 7. international Conference on Amorphous and Liquid Semiconductors*, ed. by Spear W.E., (CICL, University of Edinburgh 1977) pp. 437.
- [22] Moustakas T.D., Lewis A.J., Poul W., *Solid State Commun.* Vol. 20 pp. 969-970, 1976.
- [23] Lecomber P.G., Spear W.E., Kalbitzer S., Muller G., *Proceedings of the 7. international Conference on Amorphous and Liquid Semiconductors*, ed. by Spear W.E., (CICL, University of Edinburgh 1977) pp. 442.
- [24] Lecomber P.G., Spear W.E., Kalbitzer S., Muller G., *J. Non-Cryst. Solids*, Vol. 35, pp. 327-339, 1980.
- [25] Lecomber P.G., Spear W.E., Kalbitzer S., Muller G., *Phil. Mag.*, Vol. B 41, pp. 439-449, 1980.
- [26] Lecomber P.G., Spear W.E., Kalbitzer S., Muller G., *Phil. Mag.*, Vol. B 39, pp.159-164, 1979.
- [27] Beyer W., Fisher R., *Appl. Phys. Lett.* Vol. 31 pp. 850-851, 1977.
- [28] Taniguchi M., Hirose M., Osaka Y., *J. Crystal Growth* Vol. 45, pp. 126-128, 1978
- [29] Sol N., Kaplan D., Dieumegard D., Dubreuil D., *J. Non-Cryst. Solids*, Vol. 35, pp. 291-292, 1980.
- [30] Mott N. F., *Adv. Phys.* Vol. 16 pp. 49-50, 1967.
- [31] Cohen M. H., Fritzsche H., Ovshinsky S. R., *Phys. Rev. Lett.* Vol. 22:65 1969.
- [32] Mott N. F., *Phil. Mag.*, Vol. 19, pp. 835-839, 1969.
- [33] Akkaya A., *M.S. Thesis*, pp.13, 1993.
- [34] Oheda H., *J. Appl. Phys.* Vol. 52, pp. 6693-6695, 1981.